UPPSALA
UNIVERSITET

Digital Comprehensive Summaries of Uppsala Dissertations from the Faculty of Science and Technology 265

Isotopes as Mechanism Spies

Nucleophilic Bimolecular Substitution and Monoamine Oxidase B Catalysed Amine Oxidation Probed with Heavy Atom Kinetic Isotope Effects

SUSANNA MACMILLAR

ACTA
UNIVERSITATIS
UPSALIENSIS
UPPSALA
2006

ISSN 1651-6214
ISBN 978-91-554-6776-8
urn:nbn:se:uu:diva-7441

Dissertation presented at Uppsala University to be publicly examined in B22, BMC, Husargatan 3, Uppsala, Saturday, January 27, 2007 at 09:15 for the degree of Doctor of Philosophy. The examination will be conducted in English.

Abstract
MacMillar, S. 2006. Isotopes as Mechanism Spies. Nucleophilic Bimolecular Substitution and Monoamine Oxidase B Catalysed Amine Oxidation Probed with Heavy Atom Kinetic Isotope Effects. Acta Universitatis Upsaliensis. *Digital Comprehensive Summaries of Uppsala Dissertations from the Faculty of Science and Technology* 265. 93 pp. Uppsala.
ISBN 978-91-554-6776-8.

This thesis concerns the study of reaction mechanisms by means of kinetic isotope effects (KIEs). Studies of the nucleophilic bimolecular substitution (S_N2) reaction had the dual purpose of improving our fundamental understanding of molecular reactivity and assessing the ability of kinetic isotope effects to serve as mechanistic tools. The transition state of the S_N2 reaction between a cyanide ion and ethyl chloride in tetrahydrofuran was found to be reactant like and only slightly tighter than has been found previously for the same reaction in dimethyl sulphoxide. One conclusion was that the transition-state structure in this reaction was predicted fairly well by the theoretical calculations, even without solvent modelling. The S_N2 reactions between cyanide ions and *para*-substituted benzyl chlorides were found to have reactant-like transition states, of which the C_α-Cl bond was most influenced by the *para*-substitution. Theoretical calculations indicated that the chlorine KIEs could be used as probes of the substituent effect on the C_α-Cl bond if bond fission was not too advanced in the transition state. Furthermore, the nucleophile carbon $^{11}C/^{14}C$ KIEs were determined for the reactions between cyanide ions and various ethyl substrates in dimethyl sulphoxide.

Precision conductometry was employed to estimate the aggregation status of tetrabutylammonium cyanide in tetrahydrofuran and in dimethyl sulphoxide, which is of interest as tetrabutylammonium cyanide is frequently used as the nucleophilic reagent in mechanistic investigations and synthetic reactions. The tendency for ion-pair formation was found to be very slight, significant, and very strong in dimethyl sulphoxide, water, and tetrahydrofuran, respectively.

The nitrogen kinetic isotope effect on monoamine oxidase B catalysed deamination of benzylamine was determined in an attempt to obtain conclusive evidence regarding the mechanism of the oxidation. Monoamine oxidase is an important drug target in connection with the treatment of, for example, depression and Parkinson's disease, and knowledge on how the enzyme effects catalysis would facilitate the design of highly selective and efficient inhibitors.

Keywords: nucleophilic bimolecular substitution/SN2, kinetic isotope effects, precision conductometry, monoamine oxidase B/MAO B, reaction mechanism, carbon 11C/14C kinetic isotope effect, ion pairing/triple-ion formation, para-substituted benzyl chlorides, tetrabytylammonium cyanide

Susanna MacMillar, Department of Biochemistry and Organic Chemistry, BMC, Box 576, Uppsala University, SE-75123 Uppsala, Sweden

ISSN 1651-6214
ISBN 978-91-554-6776-8
urn:nbn:se:uu:diva-7441 (http://urn.kb.se/resolve?urn=urn:nbn:se:uu:diva-7441)

The cloudcapp'd towers, the gorgeous palaces,
the solemn temples, the great globe itself,
Yea, all which it inherit, shall dissolve.
And like this insubstantial pageant faded,
leave not a rack behind:
We are such stuff as dreams are made on,
And our little life is rounded with a sleep.

The Tempest, Act IV, Scene 1
William Shakespeare

Till Mamma och Pappa

List of Papers

This thesis is based on the following papers, which are referred to in the text by their Roman numerals.

I Fang, Y-r.; MacMillar, S.; Eriksson, J.; Kołodziejska-Huben, M.; Dybała-Defratyka. A.; Paneth. P.; Matsson, O.; Westaway, K. C. The Effect of Solvent on the Structure of the Transition State for the S_N2 Reaction between Cyanide Ion and Ethyl Chloride in DMSO and THF Probed with Six Different Kinetic Isotope Effects. *J. Org. Chem.* **2006**, *71*, 4742-4747.

II Westaway, K. C.; Fang, Y-r.; MacMillar, S.; Matsson, O.; Islam, S. M.; Poirier, R. A. A New Insight into Using Chlorine Leaving Group and Nucleophile Carbon Kinetic Isotope Effects to Determine Substituent Effects on the Structure of S_N2 Transition States. *Submitted manuscript.*

III MacMillar, S.; Matsson, O. The Nucleophile Carbon $^{11}C/^{14}C$ Kinetic Isotope Effects for the Reactions between Cyanide Ions and Ethyl Substrates in DMSO. *Technical note.*

III MacMillar, S.; Fang, Y-r.; Westaway, K. C.; Matsson. O.; Beronius, P. Solvent Effects on Ion Pairing of Tetrabutylammonium Cyanide. A Conductometric Study. *Submitted manuscript.*

IV MacMillar, S.; Edmondson, D. E.; Matsson, O. Nitrogen Kinetic Isotope Effects as Probes of the Mechanism of Monoamine Oxidase B. *Manuscript.*

Contents

Abbreviations & Acronyms

‡	(superscript) relate to transition state
Å	Ångström, 10^{-10} m
a.c.	alternating current
anhydr.	anhydrous
aq.	aqueous
Bn	benzyl
Bq	Becquerel
Bu_4NCN	tetrabutylammonium cyanide
c	concentration
c_0	critical concentration limit for triple-ion formation
D	deuterium
d.c.	direct current
DH theory	Debye-Hückel theory
DMSO	dimethyl sulphoxide
e	elementary charge
E_a	activation energy
EIE	equilibrium isotope effect
ESI	electrospray ionization
Et	ethyl
eV	electron volt
EXC	isotope effect contributions from exited vibrational levels
FAD	flavin adenine dinucleotide
FHFP	Fuoss, Hsia, Fernandez-Prini
f_m	mole fraction
h	Planck's constant
HAKIE	heavy atom kinetic isotope effect
HEPES	4-(2-hydroxyethyl)piperazine-1-ethanesulphonic acid
HPLC	high performance/pressure liquid chromatography
I	electric current or ionic strength
IRMS	isotope ratio mass spectrometry
k	rate constant
K	equilibrium constant
k_B	Boltzmann's constant
k_{cat}	turnover number
K_{cell}	cell constant
KIE	kinetic isotope effect

KIE_T	contribution to the isotope effect from tunnelling
K_M	apparent dissociation constant
K_p	equilibrium constant for ion-pair formation
LG	leaving group
MAO	monoamine oxidase
Me	methyl
MMI	contribution to the isotope effect from masses and moments of inertia
MS	mass spectrometry
NMR	nuclear magnetic resonance
Nu	nucleophile
OTs	tosylate
PS	product state
q	critical distance for ion-pair formation according to Bjerrum's theory
QSAR	quantitative structure-activity relationship
R	resistance
R	gas constant
r. c.	reaction coordinate
RS	reactant state
SET	single-election transfer
S_N2	bimolecular nucleophilic substitution
T	temperature in K
t	temperature in ºC
$t_{½}$	half-life
TDF	temperature-dependent factor
THF	tetrahydrofuran
TIF	temperature-independent factor
TLC	thin-layer chromatography
TS	transition state
UV	ultra-violet
V	electric potential difference, voltage, or maximum velocity of catalysis
v	velocity
VP	isotope effect contributions from the normal mode vibrational frequencies
z	ion charge
ZPE	zero point energy or contributions to the isotope effect from zero point energies
α	degree of dissociation
β^-	negatron/electron
β^+	positron
γ	mean ionic activity constant
$\Delta G^‡$	Gibb's free energy of activation

$\Delta H^{\ddagger}$	enthalpy of activation
$\Delta S^{\ddagger}$	entropy of activation
ε	dielectric constant
η	viscosity
κ	conductivity
Λ	equivalent conductivity
Λ_0	equivalent conductivity at infinite dilution
Λ_m	molar conductivity
ν	frequency

1 Introduction

The work presented in this thesis concerns the study of reaction mechanisms by means of kinetic isotope effects. Nucleophilic bimolecular substitution reactions were studied to both increase our understanding of fundamental molecular reactivity and to assess the ability of kinetic isotope effects to serve as mechanistic tools. The reactions were observed upon variation of the solvent (Paper I) and substitution of the substrate (Paper II) and leaving group (Paper III). Furthermore, precision conductometry was employed to estimate the aggregation status of tetrabutylammonium cyanide in tetrahydrofuran and in dimethyl sulphoxide (Paper IV). The aggregation status of tetrabutylammonium cyanide is of interest as it is frequently used as the nucleophilic reagent in mechanistic investigations (e.g. Papers I-III) and synthetic reactions. The nitrogen kinetic isotope effect on monoamine oxidase B catalysed deamination of benzylamine was determined in an attempt to obtain conclusive evidence for the mechanism of oxidation (Paper V). As monoamine oxidase is of great interest as a drug target in connection with diseases such as depression and Parkinson's disease, it is of great importance to ascertain how the enzyme pursues catalysis. The design of highly selective and efficient inhibitors would be facilitated by such knowledge.

2 Kinetic Isotope Effects

The substitution of an atom in a molecule by one of its isotopes can alter the rate at which the molecule reacts. The kinetic isotope effect (KIE) is defined as the ratio of the reaction rates, according to Equation (2.1),

$$\mathrm{KIE} = k_{\mathrm{light}} / k_{\mathrm{heavy}} \qquad (2.1)$$

where k_{light} is the rate constant for the molecule containing the light isotope and k_{heavy} is the rate constant for the molecule with the heavy isotope. Isotopic substitution is the most subtle alteration possible as only the mass is altered (the change in nuclear spin is not considered). By using this method to study a reaction the mechanism will not be affected, as may be the case when structure-reactivity correlations are used.[1] The presence or lack of a KIE can be used to identify rate-limiting steps, and the structural features of the activated complex can be inferred from the magnitude of the effect. Kinetic isotope effects are classified according to the position of the isotopically substituted atom.

- Primary KIEs result when bonds to the isotopically substituted atom are formed or broken in either the rate-limiting step or in the pre-equilibrium of a reaction.

- Secondary KIEs result when the isotopically substituted atom influences the reaction rate but does not take part in the bond breaking/formation process.

- Solvent KIEs occur when the reaction rate is affected by the isotopic composition of the solvent.

2.1 The Transition State

The rate constant for a reaction comprised of one elementary step is governed by the amount of energy that has to be surpassed when reactants are transformed into products. Indeed, the Arrhenius equation (Eq. 2.2),

which is based on experimental results, shows that the activation energy, E_a, together with temperature, T, and the pre-exponential factor A, governs the rate constant, *k*, and thus the rate of the reaction. *R* is the gas constant.

$$k = Ae^{-E_a/RT} \qquad (2.2)$$

The idea of a transition state[2] (TS) as the position highest in energy along the reaction pathway was the starting point for what has become the transition-state theory.[3,4] Figure 2.1a shows the energy potential profile for an elementary step, the transition state of which is denoted $X^{\ddagger}$. This is a common form of two-dimensional representation of the reaction path, which in reality is the minimum-energy path situated on a multi-dimensional potential energy hypersurface. The TS on such a surface is in fact not a maximum but, as Figure 2.1b illustrates, a saddle point.

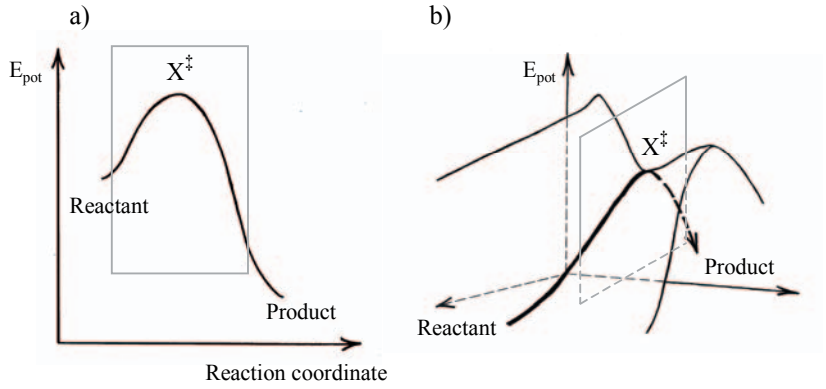

Figure 2.1 a) The energy potential profile (EPP) of an elementary step where the position of the TS is indicated by $X^{\ddagger}$. b) A three-dimensional potential energy surface with the vertical cut (in grey) through the surface that constitutes the EPP.

In TS theory the activated complex,[5] which is the physical entity passing through the transition state, is assumed to be in equilibrium with the reactants, see Figure 2.2.

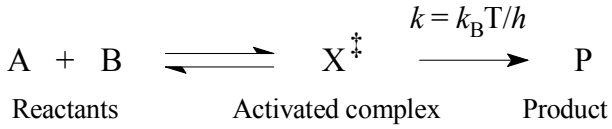

Figure 2.2 The kinetic scheme for the activated complex.

The difference in Gibbs' free energy between the reactant state and the transition state, $\Delta G^{\ddagger}$, regulates the rate constant of the elementary reaction by the relation given in Eq. (2.3). The universal rate constant for the

decomposition of the TS, $k_B T/h$, is comprised of Boltzmann's constant, k_B, Planck's constant, h, and the absolute temperature, T.

$$k = \frac{k_B T}{h} e^{-\Delta G^{\ddagger}/RT} \qquad (2.3)$$

Equation (2.4) shows the relation between $\Delta G^{\ddagger}$ and the two other parameters of activation: the enthalpy of activation, $\Delta H^{\ddagger}$, and the entropy of activation, $\Delta S^{\ddagger}$. The difference between the enthalpy of activation and the activation energy as defined by Arrhenius is, as Eq. (2.5) makes clear, the term RT. At room temperature this term is very small and in such cases E_a and $\Delta H^{\ddagger}$ can be equated.

$$\Delta G^{\ddagger} = \Delta H^{\ddagger} - T\Delta S^{\ddagger} \qquad (2.4)$$

$$E_a = \Delta H^{\ddagger} + RT \qquad (2.5)$$

The description of an activated complex is often based on the structural features of the reactants and products. This is a relevant comparison since the Hammond postulate[6] states that two states (reactant and transition or transition and product) of an elementary reaction that are of similar energy should only need a minor structural reorganization in order to interconvert. Thus, an exothermic reaction will have a reactant-like transition-state structure, whereas a product-like TS structure would be expected for an endothermic reaction. One way of representing the relation between energy and structure for an activated complex is the reaction coordinate diagram, as presented by More O'Ferrall and Jencks.[7,8] In essence, this type of diagram is a top view of a three-dimensional potential energy surface where the energy is perpendicular to the plane of the paper. As can be seen in Figure 2.3, the two axes represent bond breaking/formation of the reacting system, which in this case undergoes the substitution of X for Y.

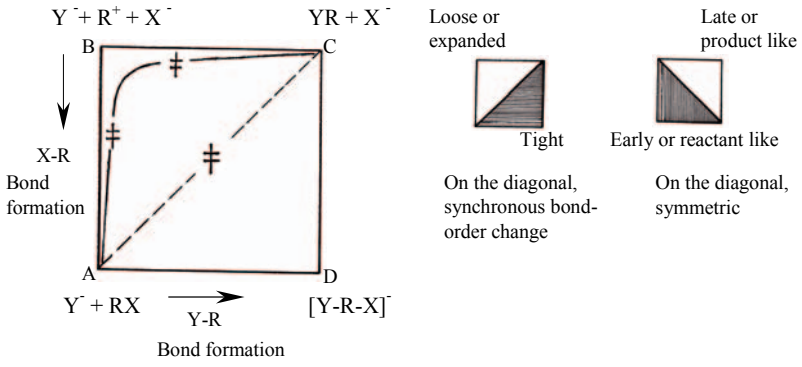

Figure 2.3 The More O'Ferrall-Jencks diagram of a substitution reaction and the corresponding terms used to describe the TS structure.

In Figure 2.3, the dashed line represents an S_N2 reaction (for details see Chapter 4), with its TS halfway between points A and C. If the energy of the product molecule is increased, the TS will be moved towards the product side, point C, and thus the TS structure will become more product-like or 'late'. On the other hand, increasing the energy of the starting material, RX, will give a reactant-like or 'early' TS structure. The change in overall bond order for the R fragment of the activated state will be preserved if the change in bond order to X and Y is synchronous. Transition states of such constitutions will be found on the diagonal from point A to point C. The diagonal between points B and D indicates the position of so-called symmetric structures, in which the R fragment has an equal amount of bond order to X as to Y. Increased overall bond order renders a tight TS structure, whereas a decrease will produce a loose structure, the latter of which ensues if the stability of R^+ is increased. A continued increase in R^+ stability will move the TS closer to point B, ending up with a reaction borderline to S_N1. Eventually, if R^+ is stable enough to exist on its own, the TS will become an intermediate in the S_N1 mechanism, as shown by the dotted line in Figure 2.3.

Although the More O'Ferrall-Jencks diagrams are useful for keeping track of TS structure nomenclature and structure-energy relationships, it should be remembered that they are just three-dimensional representations of processes that are multi-dimensional. [9]

2.2 The Origin of Kinetic Isotope Effects

As the rate of a reaction is a consequence of the difference in energy between the reactant state and its transition state, the KIE will be an expression of the energy difference in the transition from reactant to activated complex for two isotopologues. According to the so-called semiclassical theory,[10] the KIE may be expressed as a product of three factors reflecting the origin of this energy difference, see Eq. (2.6).

$$k_{light}/k_{heavy} = \text{KIE} = \text{MMI}\times\text{EXC}\times\text{ZPE} \qquad (2.6)$$

Each factor in Eq. (2.6) constitutes of the ratio of the isotopic transition states to that of the isotopic reactant states with regard to masses and moments of inertia (MMI) through translational and rotational energies, excited vibrational modes (EXC) and the zero point energies of the vibrational modes (ZPE). The zero point energy is the lowest potential

energy allowed as a consequence of the Heisenberg uncertainty relation. This treatment of KIEs presupposes, among other things,[11] that translational, rotational and vibrational modes of motion can be divided into and treated as independent contributions, and that the Born-Oppenheimer approximation, which infers that isotopic substitution of a molecule does not alter its electronic potential energy, is valid. All three factors in Eq. (2.6) can be expressed as functions of the vibrational frequencies of the reactant and transition states, of which the transition state is devoid of its reaction coordinate motion. (The reaction coordinate is the normal mode along which the activated complex decomposes.)

The dominant factor for hydrogen KIEs is usually the ZPE factor. Figure 2.4 illustrates proton or deuteron transfer from an acid to a base, and the resulting primary (1º) KIE. The vibrations most affected by isotopic substitution will be the two stretching modes, of which the asymmetric stretch is along the reaction coordinate and can be seen as a translational movement of the transferred atom. The potential energy of the stretch for the reactant state (RS) and the symmetric stretch of the TS are represented by parabolas in Figure 2.4, and the zero point energies are indicated.

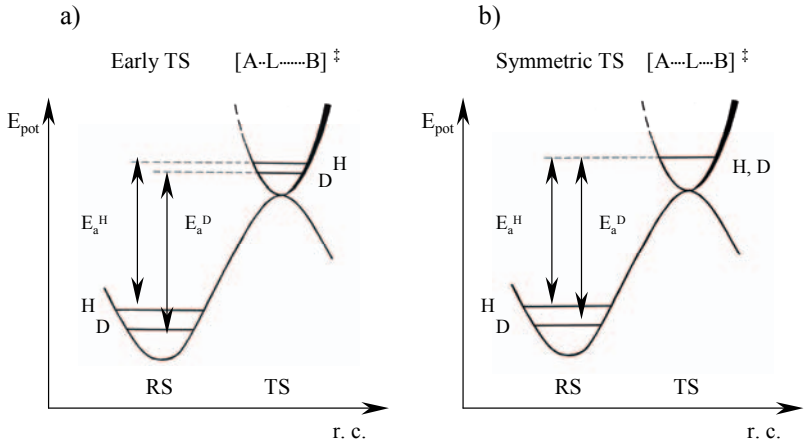

Figure 2.4 The 1º KIE for proton transfer between an acid and a base interpreted by means of zero point energies. The isotopically labelled position is denoted L. a) The isotopic energy differences of an early TS. b) The isotopic energy differences of a symmetric TS.

The difference in ZPE will produce a KIE as the activation energy of the molecule containing the heavy atom will be greater than the activation energy of the light isotopologue. If the TS is early, as in Figure 2.4a, the A-L bond will only be slightly ruptured and the vibrational frequencies of the TS symmetric stretching mode will be dependent on the mass of L. The resulting difference in the isotopic ZPE in the TS will to some extent compensate the isotopic ZPE difference in the RS, and the difference in the isotopic activation energies will be decreased. The resulting KIE will thus be

lower than would be expected by considering only the isotopic ZPE difference in the RS. Similarly, a late TS will decrease the KIE, but in this case, the decrease will arise from the increased influence of the L-B bond. If the frequency of the symmetric stretching vibration of the TS is independent on isotopic substitution, the difference in isotopic ZPE in the RS will be fully expressed in the KIE. This is the case when the transferred atom is bound with equal strength to the donor and the acceptor, as in Figure 2.4b. As predicted by Westheimer and Melander,[12,13] a maximum 1º KIE for transfer reactions will be seen if the TS is symmetrical. The magnitude of such a maximum for a 1º D KIE is estimated to be 7–10.[13,14]

The magnitude of a secondary (2º) hydrogen/deuterium KIE is considerably smaller than that of a 1º KIE, at most reaching 1.25 per D.[15,16] Secondary KIEs are mainly caused by changes in the force constant for vibrations other than in the reaction coordinate mode. Figure 2.5 shows the formation of a carbocation from an alkyl halide and the potential energies of a bending vibration for the reactant and the transition state. The labelled position is denoted L and the parabolas represent the potential energies. As the isotopically substituted atom is bound to one of the atoms participating in the bond fission it is classified as a 2º-α KIE.

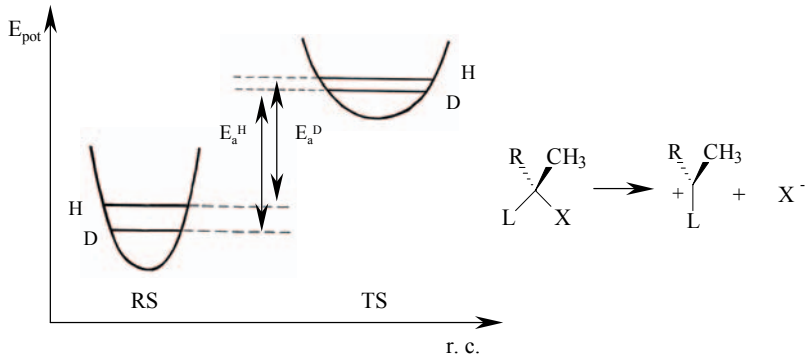

Figure 2.5 The 2º-α KIE for the formation of a carbocation from an alkyl halide. The isotopically labelled position is denoted L. R denote an arbitrary alkyl group.

When the carbocation is formed, the bending modes of the C-L bond will become looser. Thus, the potential representing the TS will be softer than that for the RS. A softer potential is accompanied by a smaller difference in the isotopic zero potential energies. The resulting higher activation energy of the molecule with the heavy isotope will produce a KIE greater than unity; usually referred to as a *normal* KIE. If the opposite occurs, i.e. the TS has a harder energy potential surface than the RS, the KIE will become less than unity or so-called *inverse*. Inverse KIEs (primary as well as secondary) are expected whenever there is an increase in bond order or an increase in steric

hindrance to the bending motion of the isotopic atom in the TS compared to the RS.

If the hydrogen atoms in the methyl groups of the alkyl halide shown in Figure 2.5 were to be isotopically substituted, the resulting KIE would be classified as a 2º-β KIE. This type of KIE is sensitive to the amount of charge built up on the atom undergoing bond breaking/formation. The influence on the reacting centre exerted by the isotopically substituted atom(s) is largely attributed to hyperconjugation, but inductive effects also contribute.[16]

KIEs caused by isotopic substitution of elements other than hydrogen are called heavy atom kinetic isotope effects (HAKIEs). As the maximum KIE possible for a certain element is determined by the relative difference in mass between the two isotopes, HAKIEs seldom exceed 10% (i.e. a KIE of 1.1).[17] Isotopic substitution of heavy atoms results in a vibrational energy difference that is less than that resulting from the isotopic substitution of hydrogen atoms. The effect on mass and moment of inertia is, however, of a similar magnitude. Thus, the contribution from the MMI factor may be considerable, making it impossible to interpret the KIE according to the ZPE approximation. In some cases, the balance between all three factors (MMI, EXC and ZPE) determines the HAKIE. It may therefore be necessary to employ theoretical calculations in order to establish the connection between the observed KIE and the structural features of the TS.[18,19]

In the TS theory presented above and in the KIE expression of Eq. (2.6) it is assumed that all the reacting molecules proceed from the reactant state to the product state via the transition state. However, in some cases, quantum tunnelling (i.e. passage through the reaction barrier to the RS) must be considered. In order to fit the semiclassical KIE theory, the reaction barrier, which is approximated to a parabolic shape, must have a soft curvature. In the case of narrow or steep reaction barriers (i.e. the reaction coordinate motion has a high frequency) Eq. (2.6) must be corrected for tunnelling. This can be done by multiplying the right-hand expression of Eq. (2.6) by a tunnelling correction factor. Apart from narrow reaction barriers, tunnelling is favoured by low temperature and light nuclei. Tunnelling can increase the magnitude of hydrogen KIEs substantially, not only if the hydrogen atom itself is moving along the reaction coordinate (as in 1º KIEs) but also, for example, if there is coupling between the vibrational modes of the α-hydrogens (2º KIEs) and the reaction coordinate movement.[20,21] However, tunnelling is not a phenomenon exclusive to hydrogen KIEs. A relatively modest tunnelling contribution in absolute terms can have a significant impact on a HAKIE since the latter has a small magnitude.[18]

2.3 Kinetic Complexity

So far, only elementary reactions have been considered. When dealing with multi-step reactions the observed reaction rate depends on the rate of one or several of the constituting elementary steps. The step that contributes most to the overall rate expression is called the rate-limiting step.* Consider the reaction sequence shown in Figure 2.6, where A and B reversibly form the reaction intermediate C, which combines with D to produce the overall product. The overall rate, v, is here expressed according to the steady-state approximation, which implies that the intermediate is consumed as it is formed. If the second step in the reaction sequence is significantly faster than the first step, i.e. $k_2[D] >> k_{-1}$, the observed rate is solely dependent on k_1, which is thus the rate-limiting step. Conversely, if the back flux of C to A and B is faster than the forward reaction to the product, i.e. $k_{-1} >> k_2[D]$, then the overall reaction rate will be limited by the second step.

$$A + B \underset{k_{-1}}{\overset{k_1}{\rightleftharpoons}} C \qquad v = \frac{k_1 k_2 [A][B][D]}{k_{-1} + k_2 [D]}$$

$$C + D \xrightarrow{k_2} \text{Product}$$

if $k_2[D] >> k_{-1}$ $\quad v = k_1[A][B]$ $\quad k_{obs} = k_1$ $\quad$ Step 1 RLS

if $k_2[D] << k_{-1}$ $\quad v = \frac{k_1 k_2}{k_{-1}}[A][B][D]$ $\quad k_{obs} = \frac{k_1 k_2}{k_{-1}}$ $\quad$ Step 2 RLS

Figure 2.6 The reaction scheme for the reaction between A and B which, via intermediate C and reactant D, forms the product, together with the accompanying microscopic rate constants for the elementary steps k_1, k_{-1} and k_2. The overall rate expression is derived in accordance with the steady-state approximation. The rate constant for the observed rate, k_{obs}, and the rate-limiting step (RLS) is given for two possible scenarios.

In the discussion above, $k_2[D]$ was considered to be a pseudo-first-order rate constant as would be the case, for example, for solvolysis. However, it should be noted that a reactant entering the reaction at an intermediate step, such as D, can cause a shift in the rate-limiting step simply due to a change in its concentration.[22]

The observed KIE is determined by the size of the intrinsic KIE (i.e. the KIE of a particular reaction step) and the degree to which the isotopically sensitive step limits the overall rate of the reaction. A small KIE or none at

* It has been recommended that the terms rate-limiting, rate-determining and rate-controlling step be used as synonyms, according to the IUPAC Recommendations of 1994, although some distinctions are mentioned. Muller, P. *Pure. Appl. Chem*. **1994**, *66*, 1077-1184.

all can thus be the consequence of a lack of sensitivity to isotopic substitution, or the fact that the reaction step sensitive to isotopic substitution does not contribute sufficiently to the observed rate. Although complicating the situation, at times this makes KIEs an excellent tool for the detection of shifts in rate-limiting steps.[23]

2.3.1 Enzymatic Reactions

A simplified version of a reaction scheme for an enzymatic reaction is presented in Figure 2.7. The enzyme and substrate reversibly form an enzyme-substrate complex, which undergoes chemical conversion according to the rate constant k_2. The ensuing enzyme-product complex then collapses to give rise to the free product and enzyme with the rate constant k_3.

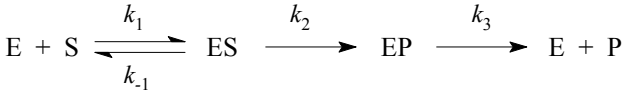

Figure 2.7 A simplified representation of an enzymatic reaction where E, S and P denote the enzyme, substrate and product, respectively.

In many cases the chemical transformation strongly limits the reaction rate, but there are also examples of enzymes being limited only by the supply of substrate, i.e. diffusion control, or the release of product. Enzyme kinetics measurements made under steady-state conditions, that is, when the substrate is in large excess and the concentration of the reaction intermediates can be assumed to be constant, provide information on three parameters: k_{cat}, K_M and k_{cat}/K_M.

- k_{cat} is the catalytic constant, or the so-called turnover number, which represents the maximum amount of substrate molecules converted to product per active site per unit time. At saturating conditions the maximum velocity of catalysis, V, equals k_{cat} multiplied by the total enzyme concentration.
- K_M is the apparent dissociation constant for all enzyme-bound species. Furthermore, K_M is equal to the substrate concentration at which half the maximum velocity of catalysis is achieved.
- Their ration, k_{cat}/K_M, sometimes called the specificity constant, is an apparent second-order rate constant that allows the specificity of competing substrates to be compared. At low substrate concentrations it describes the catalytic efficiency.

Kinetic isotope effects on enzymatic reactions can be determined either by direct comparison of the reaction rates (the so-called direct or non-competitive method) or by competitive kinetics, where both isotopic substrates are present at the same time (the competitive method).[24] The direct method provides all three catalytic parameters mentioned above and thus enables the calculation of the isotope effect on one turnover, $^{D}k_{cat}$ or ^{D}V in the case of a deuterium effect, or on all steps between free reactants and the first irreversible step, $^{D}(V/K_M)$ or $^{D}(V/K)$. The competitive method however, only provides the value of V/K. In most cases the direct method is not a realistic alternative when dealing with heavy atom KIEs as these are too small compared with the errors in the rate determination.

2.3.2 Multiple Isotope Effects

When studying a reaction mechanism it is essential to understand the order of the constituting steps, or indeed, if the reaction is concerted. As mentioned above, the observed KIE is a consequence of the amount of rate limitation of the step sensitive to isotopic substitution and the intrinsic KIE of that step. In multiple isotope effects[*] isotopic substitution is used to change the degree to which a specific step in a reaction contributes to the overall rate. As an example, let us consider a reaction comprised of the formation of one nitrogen-carbon bond and the transfer of a proton. The nitrogen KIE and the deuterium KIE have been determined, but one question still remains: Are the two steps concerted or does the proton transfer precede nitrogen-bond formation? Re-determining the nitrogen KIE[**] in the presence of deuterium can provide the answer, as the nitrogen KIE will be affected differently depending on the timing of the steps in the reaction. The free-energy diagrams for the two scenarios are presented in Figure 2.8 together with the notation used to describe the sensitivity of the reaction step(s) to isotope substitution.

[*] Multiple isotope effects are sometimes referred to as "the double isotope fractionation test." It should also be noted that the term "multiple isotope effect" is not used exclusively in this context but also for the independent determination of several KIEs on the same reaction system.

[**] The notation of the spectator isotope is usually applied as a lower case index after the KIE. For example, if a nitrogen KIE on an enzyme-catalysed reaction determined under competitive conditions is noted $^{15}(V/K)$, the nitrogen KIE upon deuteration will be denoted $^{15}(V/K)_D$.

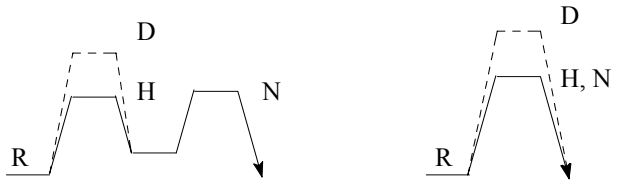

Stepwise; proton transfer preceding the nitrogen-bond formation

Concerted

Figure 2.8 The free energy diagrams for two possible reaction scenarios. R denotes the reactant state and H and N denote the isotopic sensitivity of the steps for hydrogen and nitrogen, respectively. The dashed lines represent the free energy following deuterium substitution.

The observed nitrogen KIE in the stepwise scenario as presented in Figure 2.8 will be reduced as the proton transfer step will be more rate limiting upon deuterium substitution. Conversely, no change in the nitrogen KIE would be expected in the concerted case as the single reaction step completely determines the overall reaction rate. However, should the concerted step be part of a more complex mechanism, an increase in the nitrogen KIE may be observed upon deuterium substitution if the nitrogen and hydrogen sensitive step were not fully rate limiting compared with the other steps. The intention of the example given above is merely is to present the principle of multiple isotope effects. When applied to more complex systems the possibility of isotopic substitution affecting more than one step in a mechanism must also be taken into account. However, the order of the steps in a reaction has been successfully elucidated in both enzymatic and non-enzymatic reactions.[25-27]

In the example discussed above, the dependency of a heavy atom KIE is studied upon deuterium substitution, which is the most commonly used combination. In principle, substitution of any element may be employed. The combination of two heavy atom KIEs would, however, be impractical due to the small magnitudes of isotope effects. If the combination of two deuterium or tritium KIEs is studied and both isotopic positions are affected in the same step then the coupling between the motions of the two hydrogen atoms in the transition state must be considered.[28] In such cases the isotope effects may become synergetic as the isotopic substitution in one position may affect the tunnelling contribution to the KIE of another isotopic position.

3 Equilibrium Isotope Effects

The equilibrium isotope effect (EIE) is defined as the ratio of equilibrium constants according to Eq. (3.1), where K_{light} is the equilibrium constant for the molecule containing the light isotope and K_{heavy} is the equilibrium constant for the molecule with the heavy isotope.

$$K_{light}/K_{heavy} = EIE = MMI \times EXC \times ZPE \qquad (3.1)$$

Equation (3.1) bears strong resemblance to the expressions for the kinetic isotope effect in Eqs. (2.1) and (2.2), and rightfully so, as they share a common theoretical origin.[14,17] The corresponding division into contribution factors (MMI, EXC and ZPE) according to semiclassical theory can be made as for the KIE, but the transition state is replaced by the product state, which will include all vibrational modes as it is a stable molecule. As with KIEs, a normal EIE is to be expected when there is an increase in the force constants (e.g. increased bond order or steric hindrance) associated with the isotopic atom in the product state compared with the reactant state. A normal EIE implies that the heavy element is enriched in the reactant.

Although structure dependent, EIEs are seldom used for structure studies. However, they may sometimes be used to estimate the amount of product-likeness of a transition-state structure.[17,29]

3.1 Implications on Kinetic Isotope Effect Studies

Figure 3.1 depicts a stepwise reaction consisting of a pre-equilibrium between reactant A and intermediate B, and the onward reaction of B to product C. If the conversion of B into C is the rate-limiting step and the equilibrium is rapidly reversible, $k_{-1} >> k_2$, then the rate constant for the observed rate, k_{obs}, will be the product of the equilibrium constant and the rate constant for the rate-limiting step. Likewise, if the equilibrium is sensitive to isotopic substitution, i.e. there is an EIE, the observed KIE for the overall reaction will be the product of the EIE and the KIE of the rate-limiting step. The pre-equilibrium in Figure 3.1 can, for example, be the deprotonation of a potential nucleophile, which is followed by a nucleophilic

attack. In order to obtain the intrinsic KIE for the nucleophilic attack, the observed KIE must be corrected for the EIE by division.

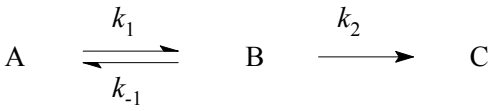

$$\text{if } k_{-1} >> k_2; \qquad k_{obs} = (k_{-1}/k_1)k_2 = K_{eq}\, k_2$$

$$KIE_{obs} = EIE \cdot KIE_{k_2}$$

Figure 3.1 The reaction scheme for a stepwise reaction consisting of a pre-equilibrium between reactant A and intermediate B and the rate-limiting conversion of B to product C. KIE_{obs} and KIE_{k2} denote the observed KIE for the overall reaction and the intrinsic KIE of the rate-limiting step, respectively.

The argument above is based on the assumption that the equilibrium is strongly in favour of the reactant A. Should this not be the case, the correction for the EIE must reflect the position of the equilibrium. In the current example this implies that if the experiment is conducted at a pH close enough to the pK_a of the potential nucleophile that significant amounts of the unprotonated nucleophile are present, this must be taken into account.[26]

$$A = 1 + (EIE - 1)f_m \qquad (3.2)$$

The correction factor, A, to be used instead of the full EIE, is given in Eq. (3.2), where f_m is the mole fraction of the protonated species.

4 Nucleophilic Bimolecular Substitution

In order to explain nucleophilic substitution at saturated carbon, Ingold and Hughes described two distinct mechanisms, which they designated S_N1 and S_N2,[30*] where S and N denote substitution and nucleophilic, respectively. The numeral represents the number of molecules that undergo covalency change in the rate-limiting step, i.e. the molecularity. Whereas the S_N1 mechanism proceeds via initial carbocation formation followed by a nucleophilic attack, the S_N2 mechanism consists of a single step in which the nucleophilic attack is concerted with fission of the bond to the leaving group. As can be seen in Figure 4.1, the central carbon of the resulting activated complex has trigonal bipyramidal geometry, which implies that there is an increase in the steric constriction in the transition state compared with the reactant state. Thus, the rate of an S_N2 reaction is sensitive to the steric bulk of the substituents on the substrate as well as the nucleophile. Moreover, the backside attack by the nucleophile on the substrate results in inversion of the configuration at the central carbon.

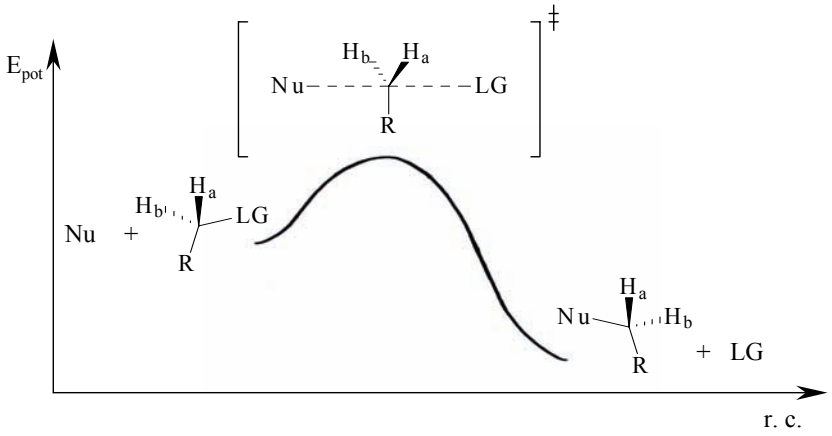

Figure 4.1 The energy potential profile and rate expression of a nucleophilic bimolecular substitution, S_N2. Nu, LG and R denote the nucleophile, the leaving group and an arbitrary alkyl/aryl group, respectively.

[*] According to the IUPAC recommendations from 1989 the S_N2 and S_N1 notation should be redesigned A_ND_N and D_N+A_N, respectively. Guthrie, R. D. *Pure Appl. Chem*. **1989**, *61*, 23-56. The S_N2 and S_N1 terminology will be used here as despite these recommendations they continue to be used frequently in mechanistic discussions.

The rate of an S_N2 reaction applies overall second order kinetics being first order in both substrate and nucleophile. Therefore, the suitability of the substrate in combination with the efficacy of the nucleophile will affect the observed rate. The choice of solvent may also be of importance, as the energy required for desolvation of the nucleophile is part of the free energy of activation. Furthermore, a strongly solvated transition state will increase the rate of the reaction, as will any structural feature of the substrate that can stabilize any partial charge at the central carbon of the activated complex.

Although conceptually simple, when subjected to deeper study nucleophilic bimolecular substitution is not as uncomplicated as may be thought at first glance. Some aspects of the reaction are not yet fully understood. The effect of substituents in, for example, the substrate or the leaving group on the transition-state structure as suggested by KIEs and Hammett ρ-values may at times be contradictory.[31] Likewise, the change in transition-state structure due to a change in solvent is not always easily predictable.[32] Further studies of the S_N2 reaction are important for the fundamental understanding of the relation between molecular structure and reactivity. Thorough knowledge of the S_N2 reaction is also essential whenever it is used as a model system in connection with enzymatic S_N2 reactions.[33]

One advantage of the S_N2 reaction is that the overall size of the reaction system (i.e. the number of participating atoms) may be sufficiently modest to allow high-level calculations of the transition-state structure and the accompanying KIEs. The combination of theoretical methods and experimental results is of advantage for both as, in the first place, theory continues to have some difficulty in making predictions for reactions involving highly energetic and strongly solvated states and secondly, there is a need for a better understanding of how the KIEs correlate with the transition-state structure.

4.1 Kinetic Isotope Effects on the S_N2 Reaction

Some of the different types of KIEs arising from isotopic substitution in the reactants of an S_N2 reaction are presented in Figure 4.2. The connection between each type of KIE and the transition-state structure will be presented briefly below.

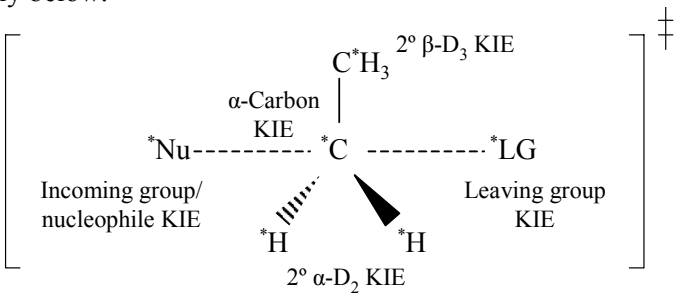

Figure 4.2 A schematic illustration of a hypothetical activated complex for the S_N2 reaction between a nucleophile and an ethyl substrate together with the positions of isotopic substitution (*) and the respective ensuing kinetic isotope effects. The use of deuterium is implied for the hydrogen KIEs.

A kinetic isotope effect can be expressed as the product of three factors: KIE_T, TIF and TDF, according to Eq. (4.1).*

$$\underset{\text{“KIE}_T\text{”}}{\text{KIE} = (k^l/k^h)_T} \times \underset{\text{“TIF”}}{(\nu^{\ddagger l}/\nu^{\ddagger h})} \times \underset{\text{“TDF”}}{(\text{VP})(\text{EXC})(\text{ZPE})} \qquad (4.1)$$

The contribution from tunnelling to the KIE is designated KIE_T. The ratio of the imaginary frequencies for the isotopic transition states constitutes the temperature-independent factor (TIF). The temperature-dependent factor (TDF) consists of the ratio of the isotopic transition states to that of the isotopic reactant states with regard to: the products of the normal mode vibrational frequencies (VP), excited vibrational modes (EXC) and zero point energies of the vibrational modes (ZPE). The superscripts l and h denote the light and heavy isotopic species, respectively.

The Incoming Group Kinetic Isotope Effect

As the imaginary frequency is higher for the species containing the lighter isotope, the temperature-independent factor will always be greater than unity. The temperature-dependent factor is determined by the change in vibrational frequencies (force constants) of the isotopically labelled atom when the reactant is converted into the transition state. An increase in binding to the isotopically labelled atom, e.g. bond formation to a nucleophile, results in increased vibrational energy in the TS compared with

* In comparison with the expression for KIE presented in Chapter 2, Eq. (4.1) includes a tunnelling contribution, and the MMI factor has been replaced by $(\nu^{\ddagger l}/\nu^{\ddagger h})(\text{VP})$.

the reactant state. Therefore, the TDF will be less than unity. The TDF will become increasingly inverse with increasing degree of bond formation in the TS. The magnitude of an incoming group KIE will thus be normal if there is a small amount of bond formation in the TS but will become inverse if bond formation is far advanced.[34-36] Due to the opposing contributions of the TIF and TDF, this type of KIE can be very small or equal to unity. The tunnelling contribution, which is always normal as tunnelling is favoured by the lighter isotope, may also be of importance, especially if the magnitude of the KIE is small.

The range of a nucleophile $^{11}C/^{14}C$ KIE has been estimated to be 1.02–0.87 for the S_N2 reaction between labelled cyanide and benzyl chloride.[34]

The Leaving Group Kinetic Isotope Effect

As the isotopically substituted atom in this case undergoes bond fission, there will be a decrease in vibrational energy as the reactant is converted into the TS. Hence the TDF will become increasingly normal with the amount of bond rupture in the TS, as will the resulting KIE. Therefore, a leaving group KIE has been regarded as indicating the advance in bond fission to the leaving group in the TS.

Recent calculations have revealed that this straightforward interpretation may not be always be valid.[19] The calculated chlorine leaving group KIEs for methyl chloride reacting with several nucleophiles remained relatively constant although the bond order of the scissile bond in the TS ranged from 0.3 to 0.7. On investigation, the TDF was found to depend, as expected, on the amount of bond fission in the TS, but in the resulting KIE this was obscured by the [$KIE_T \times TIF$] contribution, which varied randomly with the TS structure and constituted 14–40% of the KIE. The possibility of using the leaving group KIE to assess the relative change in TS structure for a series of similar substrates was, however, not dismissed as in this case the [$KIE_T \times TIF$] contribution is expected to remain relatively constant.

The maximum leaving group chlorine KIE has been estimated to be approximately 1.02.[19]

The Central Atom Kinetic Isotope Effect

The S_N2 reaction can be regarded as transfer of the central atom from the leaving group to the nucleophile. As mentioned in Section 2.2, central atom KIEs should show a bell-shaped dependence on the TS structure.[12,13] Hence, a symmetric TS will give rise to a maximal KIE, whereas an early or late TS will result in KIEs of smaller magnitudes. Indeed, this dependence has been observed not only for proton transfer but also for an α-carbon KIE.[37]

The fact that all the reported α-carbon KIEs are in the proximity of the experimental maximum KIE, which for a $^{12}C/^{13}C$ α-carbon KIE is 1.08,[38] has been described as striking. (The corresponding maxima when employing

$^{12}C/^{14}C$ and $^{11}C/^{14}C$ are 1.16[37] and 1.22,[39] respectively.) Therefore, a theoretical investigation was undertaken in an attempt to relate the α-carbon KIEs to the TS structures for the reaction between methyl chloride and several nucleophiles.[18] According to the calculations, the α-carbon KIE was very insensitive to the TS structure, i.e. the bell-shaped dependence displayed a broad maximum, and it was not possible to distinguish an early/late TS from a symmetric TS. Furthermore, none of the contributing factors given by Eq. (4.1) was observed to have a systematic relation to the TS structure. The magnitude of an α-carbon KIE can, however, be used to discriminate between different mechanisms.

The Secondary α-Deuterium Kinetic Isotope Effect

The 2º α-D KIE of an S_N2 reaction depends on the balance between an inverse contribution from the stretching modes of the C_α-H bonds and an inverse to normal contribution arising from the C_α-H bond out-of-plane bending.[16,40,41] The inverse contribution from the stretching modes is less inverse for more complex substrates (i.e. larger than methyl substrates) and largely dependent on the identity of the leaving group. The change in the force constant for the C_α-H bending is related to the nucleophile and leaving group distance as their proximity to the central carbon will compress the out-of-plane bend when the reactant is converted into the activated complex. Thus, when comparing 2º α-D KIEs for a series of substrates with the same leaving group the trend should be determined by the "looseness" of the TS. More recently, it has been argued that instead of relating the KIE to the distance between the nucleophile and the leaving group, one should consider the crowdedness of the TS, as the overall three-dimensional constriction experienced by the C_α-H bonds when bending is of importance.[42]

It has also been proposed that 2º α-D KIEs can be used to probe the symmetry of an S_N2 TS: the KIE in an unsymmetric TS is thought to be dependent only on the proximity of the nucleophile or the leaving group, whichever is the closest.[43]

A 2º α-D KIE for an S_N2 reaction is usually in the range of 0.95–1.04 per deuterium atom.[16]

The Secondary β-Deuterium Kinetic Isotope Effect

In S_N2 reactions, the 2º β-D KIEs are mainly probes of the amount of positive charge on the central carbon in the TS.[33] The developing charge is stabilized by hyperconjugation, which weakens the C_β-H(D) bonds. The 2º β-D KIE will become normal, and increasingly so with the amount of charge. There are also minor inverse contributions from inductive and steric effects, which are due to the greater electron-donating ability of D and the slightly shorter bond length of the C-D bond, respectively.[16,44]

The magnitude of a 2º β-D KIE on an S_N2 reaction is usually less than 1.05 per deuterium atom.[16]

4.2 Probing the S_N2 Transition-State Structure through Variation of Solvent, Substrate and Leaving Group (Papers I–III)

The transition-state structures of the following two S_N2 reactions were assessed with several KIEs in combination and with theoretical methods.

Paper I: cyanide ion and ethyl chloride in anhydrous tetrahydrofuran (THF) at 30 ºC.

Paper II: cyanide ion and some *para*-substituted benzyl chlorides in anhydrous THF at 20 ºC.

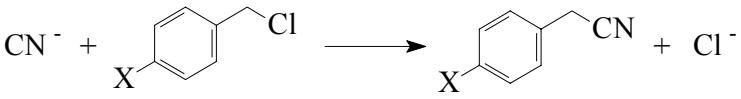

X = CH_3, H, Cl, NO_2

Furthermore, the 2º α-D_2 and nucleophile carbon $^{11}C/^{14}C$ KIEs were determined for the reactions between cyanide ion and some ethyl substrates in anhydrous and 20% aqueous dimethyl sulphoxide (DMSO) at 20 ºC. (Paper III) The determined KIEs are to be used in conjunction with theoretical methods.

LG = Br, I, OTs in anhydrous DMSO
LG = Br, I in 20% aqueous DMSO

4.2.1 The Effect of Solvent on the Transition-State Structure for the Reaction between Cyanide Ion and Ethyl Chloride (Paper I)

Recently, the transition-state structure for the S_N2 reaction between a cyanide ion and ethyl chloride in DMSO was estimated by means of both experimental KIEs and several theoretical methods.[45] Interpretation of the KIEs using the traditional (qualitative) relationships resulted in a product-like transition state with a short NC-C_α bond and a long C_α-Cl bond. Conversely, all the theoretical methods, with and without solvent modelling, predicted a reactant-like transition structure with a long NC-C_α bond and a short C_α-Cl bond. There is thus disagreement between two approaches commonly employed to elucidate transition-state structures.

In order to assess whether the lack of solvation in the calculations was a major reason for the difference between the transition-state structures predicted by theory and those interpreted from experimental KIEs in DMSO, the six previously measured KIEs were re-determined in THF. THF was chosen as solvent because: *i*) the reaction rate was fast enough to allow measurements and *ii*) although far from the gas phase,[46] it is much less polar than DMSO. Thus, THF provided the least polar reaction medium that could be employed experimentally. (The dielectric constants of DMSO, THF and the gas phase are 49, 7.3 and 1.0, respectively.)[47]

The α-carbon $^{11}C/^{14}C$ KIE in THF was determined using a chromatographic procedure in combination with liquid scintillation counting, see Table 1. (For further information on the experimental procedure, see Section 7.2.)

Table 1. *The α-carbon $^{11}C/^{14}C$ KIEs for the S_N2 reaction between tetrabutylammonium cyanide and ethyl chloride in anhydrous THF at 30 ºC.*[a]

Experiment	Sample[b]	Fraction of reaction (*f*)	R_f/R_0[c]	$(k^{11}/k^{14})_\alpha$[d]	Average
1[e]	1	0.2332	0.9486	1.2484	
	2	0.4080	0.9042	1.2376	
	3	0.5495	0.8646	1.2231	
2	1	0.5800	0.8677	1.1955	
	2	0.7221	0.8029	1.2068	
	3	0.7906	0.7582	1.2151	
3	1	0.4668	0.8939	1.2169	
	2	0.6830	0.8351	1.1860	
	3	0.7756	0.7777	1.2032	
	4	0.8182	0.7642	1.1873	
	n = 10				**1.212 ± 0.007**[f]

[a] The substrate and nucleophile concentrations in these experiments were approximately 0.05 M and 0.5 M, respectively. [b] Several samples from each experiment were analysed with regard to ethyl chloride. [c] R_f is the isotopic ratio of ethyl chloride at fraction of reaction, *f*. R_o is the isotopic ratio at 0% conversion. [d] The isotope effect was calculated using the expression $k^{11}/k^{14} = \ln(1-f)/[(1-f)(R_f/R_o)]$. [e] Experiment performed without addition of unlabelled ethyl chloride. [f] Standard deviation of the mean.

The secondary α-deuterium and β-deuterium, the α-carbon $^{11}C/^{14}C$, the nucleophile carbon $^{12}C/^{13}C$, the nucleophile nitrogen $^{14}N/^{15}N$ and the chlorine leaving group $^{35}Cl/^{37}Cl$ KIEs determined in THF and DMSO are presented in Table 2 together with the corresponding rate constants and the best set of calculated KIEs.

Table 2. *The 2º α-D_2, 2º β-D_3, α-carbon $^{11}C/^{14}C$, nucleophile carbon $^{12}C/^{13}C$, nucleophile nitrogen $^{14}N/^{15}N$ and chlorine $^{35}Cl/^{37}Cl$ leaving group KIEs and the rate constants found for the S_N2 reaction between ethyl chloride and tetrabutylammonium cyanide in anhydrous DMSO and THF at 30 ºC and the best set of KIEs calculated by theory.*

KIE	DMSO[a]	THF	KIE theory[a,b]
$(k_H/k_D)_\alpha$	0.990±0.004[c]	1.002±0.004[c]	0.994
$(k_H/k_D)_\beta$	1.014±0.003	1.003±0.005	1.005
$(k^{11}/k^{14})_\alpha$	1.208±0.019	1.212±0.021	1.17
$(k^{12}/k^{13})_{Nuc}$	1.0009±0.0007	0.9990±0.0007	0.993
$(k^{14}/k^{15})_{Nuc}$	1.0002±0.0006	1.0014±0.0003	1.0003
k^{35}/k^{37}	1.00699±0.00026	1.00659±0.00012	1.0070
$10^4\ k_H\ (M^{-1}s^{-1})$	4.22	6.58	

[a] Reference 45. [b] The KIEs quoted were calculated at the B3LYP/aug-cc-pVDZ level of theory. They represent the best set of calculated KIEs based on the absolute value of $(KIE_{DMSO} - KIE_{calc})$ for all six KIEs. [c] Standard deviation.

Upon examination of the KIEs in Table 2, only the nucleophile carbon and the chlorine leaving group KIEs are found to change significantly between the solvents DMSO and THF. The more inverse nucleophile carbon KIE in THF indicates more advanced NC-C_α bond formation in the transition state in THF than in DMSO. Meanwhile, the decrease in the leaving group chlorine KIE indicates that there is less C_α-Cl bond rupture in the transition state in THF. It should, however, be noted that these changes are very small. Compared to the maximum possible KIE for each effect, the changes in nucleophile carbon and leaving group chlorine KIEs when replacing the solvent DMSO by THF are only 3.6% and 2.1%, respectively. Thus, the changes in the nucleophile carbon and the chlorine leaving group KIEs in THF suggest that the transition state is only slightly tighter in THF.

The other KIEs do not change within the experimental errors in the measurements, and it appears that these KIEs are not sensitive enough to detect the small change in transition-state structure that occurred when the solvent was changed. However, the substantial α-carbon KIE together with the 2º α-D_2 and 2º β-D_3 KIEs confirm the S_N2 mechanism for the reaction in both solvents.

A tighter, less ionic, transition state would be expected when the solvent's ability to stabilize the ionic transition state is reduced. Thus, the direction of the observed change in transition-state structure is as expected when changing from the highly polar solvent DMSO to the less solvating THF.

Although the solvation in THF is far more extensive than that in the gas phase,[46] the great difference in polarity of the two solvents should cause a shift towards an early transition state if the difference in the transition states predicted by the two methods is mainly due to solvation. Therefore, it is highly unlikely that the absence of solvent or insufficient solvent modelling in the calculations is responsible for the different transition states that were predicted by interpreting the experimental KIEs found in DMSO and by the calculations.

The product-like transition state was originally proposed based on the magnitude of the experimentally observed chlorine KIE. In light of the recent theoretical investigation of chlorine leaving group KIEs,[19] the chlorine KIE of 1.007 could equally well be found for a reactant-like transition state. As the other KIEs are consistent with a reactant-like transition state, it now appears likely that the theoretical calculations give the most accurate transition-state structure, even in the absence of solvent modelling. The following arguments appear to support this view. The experimental value of $\Delta H^{\ddagger}$ (18.7 kcal/mol) for the reaction in DMSO was well reproduced, i.e. the deviations were 0–4 kcal/mol using several continuum solvent models.[45] Likewise, another theoretical investigation of the cyanide ion–ethyl chloride reaction in DMSO[48] afforded a value of the activation energy which, in combination with the experimental value of $\Delta S^{\ddagger}$, yields a value of $\Delta G^{\ddagger}$ that is within 1.5 kcal/mol of the experimental value. The corresponding transition structure is similar to the transition structures obtained previously with different levels of theory.[45] Another reason for favouring the transition state predicted by theoretical calculations rather than the one suggested by interpreting the experimental KIEs in the traditional manner, is that the KIEs calculated by theory for several S_N2 reactions have been close to the KIEs found experimentally.[42] Also, although outside the experimental error, the difference between the best set of KIEs calculated from the transition structures and the experimental values is small.[45] The values of $\Delta(KIE_{calc} - KIE_{exp})$ are 0.004 (α-D_2), 0.009 (β-D_3), 0.04 (α-C), 0.008 (nucleophile C), 0.0001 (nucleophile N) and 0.00001 (leaving group Cl). Thus, theory reproduces the experimental KIEs quite well even without solvent modelling. This is in line with the experimental results, which indicate that the transition-state structure is almost unaffected by the change in solvent.

The lack of change in transition-state structure with solvation found in this experimental study is supported by theoretical calculations. For example, it has been shown that adding 10 more water molecules to the S_N2 reaction between water and methyl chloride, i.e., changing the number of solvating water molecules from 3 to 13 and changing $\Delta G^{\ddagger}$ by 13.5 kcal/mol, altered the transition structure only slightly.[49] In another study of the S_N2 reaction between chloride ions and methyl chloride, it was found that microsolvation by 4 water molecules did not affect the transition structure

significantly, although the value of $\Delta G^{\ddagger}$ for the reaction changed by approximately 40 kcal/mol.[50]
The rate constant for the reaction is not very sensitive to the change in solvent as it only increases from 4.2×10^{-4} to 6.58×10^{-4} $M^{-1}s^{-1}$ when replacing DMSO by THF. The higher rate constant in THF indicates that the change in solvation is greater at the cyanide ion than at the S_N2 transition state. This is to be expected as the cyanide ion has a greater negative charge density than the charge-dispersed transition state.

It has been suggested that there are two types of S_N2 reactions with respect to the effect on the transition-state structure upon a change in solvent.[32] According to this so-called "Solvation Rule for S_N2 Reactions", a change in solvent will not affect the structure of a transition state if the nucleophile and the leaving group have the same charge. Conversely, a change in solvent will have a marked effect on the transition-state structure if the charges on the nucleophile and the leaving group are different. The results of this study on the reaction between ethyl chloride and cyanide ions are consistent with this, as changing the solvent from DMSO to THF does not alter the transition-state structure significantly.

4.2.2 Substituent Effects on the Structure of the Transition States in the Reactions between Cyanide Ions and *para*-Substituted Benzyl Chlorides (Paper II)

A recent theoretical study of the chlorine leaving group KIEs for the S_N2 reactions between methyl chloride and several nucleophiles, has questioned the straightforward use of these KIEs as indicators of the amount of fission of the bond to the leaving group in the transition state.[19] However, the chlorine leaving group KIE was thought to be potentially useful in the determination of the relative change in a TS structure for a series of similar substrates. For this reason, the 2º α-D_2, the chlorine leaving group and the nucleophile carbon $^{11}C/^{14}C$ KIEs were determined for the reactions between the cyanide ion and some *para*-substituted benzyl chlorides in THF. In addition, computational methods at three levels of theory were employed to predict the transition-state structures and the chlorine leaving group and nucleophile carbon $^{11}C/^{14}C$ KIEs. Thus, the usefulness of the nucleophile KIE as a probe of the amount of bond formation in the TS could also be assessed.

The 2º α-D_2, the central-carbon, the chlorine leaving group and the nucleophile carbon KIEs for these reactions have been determined previously in 20% aqueous DMSO or 20% aqueous dioxane.[34,43,51,52] The combined trends in the KIEs were interpreted in terms of a product-like transition state, of which the C_α-Cl bond was most influenced by the *para*-substitution. This interpretation was, however, inconclusive as the normal

nucleophile carbon KIEs indicated a low degree of bond formation in the transition states.

The nucleophile carbon $^{11}C/^{14}C$ KIEs were determined using a chromatographic procedure in combination with liquid scintillation counting, see Table 3. (For further information on the experimental procedure, see Section 7.2.)

Table 3. *The nucleophile carbon $^{11}C/^{14}C$ KIEs for the S_N2 reactions between para-substituted benzyl chlorides and tetrabutylammonium cyanide in anhydrous THF at 20 °C.*

Experiment	Sample[a]	Fraction of reaction (f)	R_f/R_0[b]	$(k^{11}/k^{14})_{Nuc}$[d]	Average
CH_3[c]					
1	1	0.3824	17.9586	1.00050	
	2	0.6023	17.9162	0.99681	
	3	0.7049	17.9137	0.99595	
2	1	0.2862	22.1123	1.00130	
	2	0.4560	22.0709	0.99893	
	3	0.5683	22.0074	0.99431	
3	1	0.4900	43.7532	1.00279	
	2	0.4637	43.8198	1.00549	
	n = 8				**0.99951 ± 0.00132**[e]
H[c]					
1	1	0.1899	17.5880	1.00651	
	2	0.2708	17.5492	1.00426	
	3	0.3946	17.5211	1.00263	
	4	0.3797	17.5048	1.00159	
2	1	0.4382	34.4559	1.00568	
	2	0.4604	34.2077	1.00738	
	n = 6				**1.00467 ± 0.00092**
Cl[c]					
1	1	0.5891	5.73601	0.99114	
	2	0.4223	5.75100	0.99615	
2	1	0.1485	22.9655	1.01569	
	2	0.2964	22.8042	1.00880	
	3	0.4375	22.7297	1.00547	
	4	0.6316	22.6741	1.00243	
3	1	0.4926	2.13424	0.99605	
	2	0.5813	2.13866	0.99894	
	3	0.7298	2.13962	0.99957	
	n = 9				**1.00158 ± 0.00249**

[a] Several samples from each experiment were analysed with regard to *para*-substituted benzyl cyanide. [b] R_f is the isotopic ratio of *para*-substituted benzyl cyanide at fraction of reaction, f. R_0 is the isotopic ratio at full conversion. [c] The substrate and nucleophile concentrations in these experiments were approximately 0.07 M (CH_3, Cl), 0.10 M (H) and 0.05 M, respectively. [d] The isotope effect was calculated using the expression $k^{11}/k^{14} = \ln(1-f)/[(1-f\,R_f/R_o)]$. [e] Standard deviation of the mean.

The 2º α-D_2 , the chlorine leaving group $^{35}Cl/^{37}Cl$ and the nucleophile carbon $^{11}C/^{14}C$ KIEs are presented in Table 4 together with the best set of calculated KIEs.

According to all levels of theory, the calculated transition structures of these reactions are reactant like. The calculations at the B3LYP/aug-cc-pVDZ level of theory, which produced the best set of KIEs, yields a transition structure in which the degrees of extension of the NC-C_α and C_α-Cl bonds are 54 and 22%, respectively, compared to the corresponding stable bonds. This is in agreement with the small change in the 2º α-D_2 KIE, which suggests that the transition states are unsymmetric or possibly symmetric and exploded.

Table 4. *The 2º α-D_2, the chlorine leaving group $^{35}Cl/^{37}Cl$ and the nucleophile carbon $^{11}C/^{14}C$ KIEs for the S_N2 reactions between some para-substituted benzyl chlorides and tetrabutylammonium cyanide in anhydrous THF at 20 ºC together with the best set of KIEs calculated by theory.*

para-substituent	$(k_H/k_D)_\alpha$ [a]	k^{35}/k^{37}	k^{35}/k^{37} theory[b]	$(k^{11}/k^{14})_{Nuc}$	$(k^{11}/k^{14})_{Nuc}$ theory[b]
CH_3	–	1.00669±0.00014[c]	1.00717	0.9995±0.0037[c]	0.9838
H	1.006±0.0009[c]	1.00591±0.00004	1.00717	1.0047±0.0023	0.9833
Cl	1.012±0.0006	1.00546±0.00016	1.00699	1.0016±0.0075	0.9825
NO_2	–	1.00556±0.00013	1.00676	–	0.9808

[a] Determined at 0 ºC. [b] KIEs calculated at the B3LYP/aug-cc-pVDZ level of theory. They represent the best set of calculated KIEs based on the absolute value of ($KIE_{exp} - KIE_{calc}$) for all four KIEs. [c] Standard deviation.

Although there are some exceptions, the general trend predicted by theory is that the chlorine leaving group KIE and the amount of bond fission in the transition state will decrease with the electron-withdrawing ability of the substituent. A decrease in the chlorine KIE is indeed observed when going from the *para*-methylbenzyl chloride to the *para*-chlorobenzyl chloride reaction, but the trend is broken by the KIE for the *para*-nitrobenzyl chloride reaction, see Table 4. In a previous study of *para*-substituted benzyl chlorides with several different nucleophiles, the chlorine leaving group KIE was found to decrease with the electron-withdrawing ability of the substituent when the nucleophile was a thiophenoxide ion, n-butyl thiolate anion or methoxide ion.[53] However, when an iodide ion was used as the nucleophile the chlorine KIE for the *para*-nitrobenzyl chloride reaction was larger than the KIE for the *para*-chlorobenzyl chloride reaction. This inconsistency of the trend in the chlorine KIEs together with the theoretical result led to a re-examination of the *para*-nitrobenzyl chloride reactions with cyanide ion and iodide ion. Analysis with HPLC showed that both reactions yielded several products, of which the S_N2 product was only a minor fraction. As the chlorine is removed from the *para*-nitrobenzyl chloride in

several different reactions, the accompanying chlorine KIE should not be considered in the present study. A plot of the observed chlorine leaving group KIEs versus the Hammett σ-values for the *para*-methyl- to the *para*-chloro substituents has a correlation coefficient of 0.982. Thus, both the calculated and the experimental chlorine KIEs indicate that the chlorine leaving group KIEs should be able to probe the substituent effect on the transition state of these S_N2 reactions. It is also worth noting that this trend in chlorine leaving group KIEs with substituent has previously been observed experimentally in several S_N2 reactions.[34,52,54]

Upon inspection of the nucleophile carbon KIEs in Table 4, it is obvious that there is no trend with a change in substituent. However, all three levels of theory suggest that the NC-C_α bond formation is more complete in the transition state and the incoming nucleophile carbon KIE becomes more inverse with the electron-withdrawing ability of the substituent. This predicted substituent effect on the length of the NC-C_α transition-state bond is consistent with the results of several experimental studies in which KIEs and Hammett ρ-values have been used to determine the substituent effect on the lengths of the Nu-C_α transition state bonds in S_N2 reactions.[34,55,56] Two of the three theoretical methods predict that the change in the NC-C_α bond formation in the transition state will be smaller than the corresponding change in the C_α-Cl bond fission. The absence of a trend in the observed data may be due to the fact that the change in the nucleophile carbon KIE is too small to be detected experimentally. It is also worth noting that although the agreement between the different levels of theory is greater in the prediction of the nucleophile KIEs, the best agreement with the experimental results is observed for the chlorine leaving group KIEs.

The overall substituent effect on the transition-state structure is thus that the transition state becomes tighter with the electron-withdrawing ability of the substituent and that the C_α-Cl bond is most affected. This is in accordance with the proposed "Bond Strength Hypothesis", which predicts that the greatest change in structure with substituent will be in the weaker reacting bond, i.e., in this case, the C_α-Cl bond.[31]

The individual contributions to the total chlorine leaving group KIEs shed light on the origin of these KIEs and have significant implications for those using these KIEs to determine the substituent effect on transition-state structure. Division of the temperature-dependent factor into the isotope effect on the vibrational energy of the reactant state $(TDF)_R$ and that on the transition state $(TDF)^‡$, made it possible to investigate their relative importance for the KIE. The chlorine leaving group KIE is mainly determined by the $(TDF)_R$, which accounts for nearly 90% of the total KIE. The small contribution of $(TDF)^‡$ to the total KIE is reasonable because the vibrational energy of the C_α-Cl bond in the transition state is small compared with that in the substrate. Moreover, the contribution from the $(TDF)^‡$ will decrease with the amount of bond fission in the transition state. It is,

however, the $[(TDF)^{\ddagger}\times TIF\times KIE_T]$ that is responsible for the decrease in the total KIE with the electron-withdrawing ability of the substituent. This means that the contribution from the $(TDF)^{\ddagger}$ term to the total KIE will be unity for a very product-like transition state and little or no substituent effect will thus be found. Therefore, the leaving group KIE will only be able to detect the substituent effect on the C_α-LG bond if the bond rupture is not well advanced in the transition state. This may be why the substituent effects on the transition-state structure are measurable for some S_N2 reactions, but not for others. For instance, the chlorine leaving group KIEs for the S_N2 reactions between the thiophenoxide ion, iodide ion and n-butyl thiolate and *para*-substituted benzyl chlorides did not change significantly with the electron-withdrawing ability of the substituent.[53] However, in the S_N2 reaction between *para*-substituted benzyl chlorides and the borohydride ion, the chlorine leaving group KIEs decreased significantly, from 1.0076 to 1.0036, with a more electron-withdrawing substituent.[54] It has been suggested that the former reactions have product-like transition states while the latter reactions have reactant-like transition states.

The results from the calculations concerning the nucleophile KIE are much less conclusive, the most striking aspect being the clearly inverse KIE for a reactant-like transition state. The total KIE is mainly determined by the balance between the strongly inverse $(TDF)^{\ddagger}$ and the normal $(TDF)_R$, and an estimate of the nucleophile KIE for an extremely early TS, i.e. $(TDF)^{\ddagger} = 1$, yielded a nucleophile $^{11}C/^{14}C$ KIE of 1.31. The use of the nucleophile KIE to determine the substituent effect on a transition-state structure clearly requires further investigation.

Considering the calculated transition structures and the very slight change in transition-state structure observed when changing the solvent from DMSO to THF (Paper I), it seems likely that the transition-state structures in the reactions between *para*-substituted benzyl chlorides and cyanide ions in aqueous DMSO or dioxane are also reactant like. This would be consistent with the normal nucleophile KIEs. The smaller chlorine leaving group KIEs and the more normal nucleophile KIEs in DMSO or dioxane, compared with the KIEs found in THF, indicate that the transition state is looser in the more polar solvents. This is to be expected as the solvent's ability to stabilize an ionic transition state is increased.

4.2.3 The Nucleophile Carbon $^{11}C/^{14}C$ Kinetic Isotope Effects for the Reactions between Cyanide Ions and Ethyl Substrates in DMSO (Paper III)

The nucleophile carbon $^{11}C/^{14}C$ KIEs for the reactions between cyanide ions and some ethyl substrates in 20% aqueous and anhydrous DMSO are presented in Tables 5 and 6, respectively.

Table 5. *The nucleophile carbon $^{11}C/^{14}C$ KIEs for the S_N2 reactions between tetrabutylammonium cyanide and ethyl iodide and bromide in 20% aqueous DMSO at 20 °C.*

Experiment	Sample[a]	Fraction of reaction (*f*)	R_f/R_0[b]	$(k^{11}/k^{14})_{Nuc}$[c]	Average
EtI[d]					
1	1	0.4009	13.599	1.00937	
	2	0.5194	13.590	1.00954	
	3	0.6140	13.592	1.01105	
	4	0.6871	13.561	1.00830	
2	1	0.4519	27.378	1.00662	
	2	0.6060	27.357	1.00667	
	3	0.7091	27.373	1.00914	
3	1	0.2801	43.195	1.00580	
	2	0.3958	43.185	1.00607	
	3	0.5077	43.214	1.00776	
	4	0.6093	43.164	1.00695	
	n = 11				**1.0079±0.0005**[e]
EtBr[f]					
1	1	0.2600	15.607	1.01017	
	2	0.4194	15.608	1.01168	
	3	0.5436	15.585	1.01103	
	4	0.6263	15.562	1.00992	
2	1	0.3819	19.046	1.00926	
	2	0.5369	19.036	1.01007	
	3	0.6522	19.019	1.01021	
	n = 7				**1.0103±0.0003**

[a] Several samples from each experiment were analysed with regard to propionitrile. [b] R_f is the isotopic ratio of propionitrile at fraction of reaction, *f*. R_0 is the isotopic ratio at full conversion. [c] The isotope effect was calculated according to $k^{11}/k^{14} = \ln(1-f)/(1-f\,R_f/R_o)$. [d] The substrate and nucleophile concentrations in these experiments were approximately 65 mM and 8.6 mM, respectively. [e] Standard deviation of the mean. [f] The substrate and nucleophile concentrations in these experiments were approximately 280 mM and 43 mM, respectively.

Table 3. *The nucleophile carbon $^{11}C/^{14}C$ KIEs for the S_N2 reactions between tetrabutylammonium cyanide and ethyl iodide, bromide and tosylate in anhydrous DMSO at 20 °C.*

Experiment	Sample[a]	Fraction of reaction (*f*)	R_f/R_0[b]	$(k^{11}/k^{14})_{Nuc}$[c]	Average
EtI[d]					
1	1	0.3531	57.7952	1.00905	
	2	0.5391	57.5676	1.00491	
	3	0.6378	57.6745	1.00887	
2	1	0.3191	73.6362	1.00660	
	2	0.4938	73.5011	1.00511	
	3	0.6529	73.4367	1.00478	
	n = 6				**1.0066± 0.0008**[e]
EtBr[d]					
1	1	0.4778	35.9029	1.00460	
	2	0.5961	35.8956	1.00497	
2	1	0.2823	33.2050	1.00865	
	2	0.4432	33.0525	1.00362	
	3	0.5341	32.9935	1.00131	
3	1	0.2940	58.3613	1.00171	
	2	0.5059	58.2813	1.00008	
	3	0.6006	58.1916	0.99756	
	n = 8				**1.0028±0.0015**
EtOTs[f]					
1	1	0.1676	62.0265	1.00586	
	2	0.2823	61.8304	1.00256	
	3	0.3974	61.6043	0.99804	
2	1	0.2357	38.0063	1.00100	
	2	0.3489	38.0437	1.00231	
	3	0.4357	37.9546	0.99933	
	n = 6				**1.0015±0.0011**

[a] Several samples from each experiment were analysed with regard to propionitrile. [b] R_f is the isotopic ratio of propionitrile at fraction of reaction, *f*. R_0 is the isotopic ratio at full conversion. [c] The isotope effect was calculated according to $k^{11}/k^{14} = \ln(1-f)/(1-f\,R_f/R_o)$. [d] The nucleophile concentrations in these experiments were 0.1 M. The substrates were added in a cumulative manner, the first addition resulting in a concentration of 0.03 M. The 2nd addition resulted in 0.015 M (EtI) and 0.03 M (EtBr). For EtI a 3rd addition yielded 0.016 M. [e] Standard deviation of the mean. [f] The substrate and nucleophile concentrations in these experiments were approximately 0.08 M and 0.1 M, respectively.

The determined nucleophile KIEs will be used together with the 2º α-D_2 KIEs in order to investigate the effect of the leaving group on the transition-state structure. Furthermore, the relation between the observed KIEs and the transition-state structures will be investigated by means of theoretical methods.

Upon inspection of Tables 5 and 6, it is evident that no significant differences can be seen for the KIEs determined in aqueous and anhydrous

DMSO. Nor can any significant changes be observed for the KIEs when different leaving groups are used. The nucleophile carbon KIEs in Table 6 are identical, within the experimental errors, to the previously determined nucleophile $^{12}C/^{13}C$ KIE for the reaction between cyanide ion and ethyl chloride of 1.0009±0.0007,[45] which corresponds to a $^{11}C/^{14}C$ KIE of 1.0027±0.0021.[39]

4.3 Conclusions and Outlook

Six different KIEs were determined for the S_N2 reaction between cyanide ion and ethyl chloride in THF. A comparison of these KIEs with those reported earlier for the same reaction in DMSO showed that the transition state is only slightly tighter in THF. Therefore, it seems unlikely that insufficient, or lack of, solvent modelling in the theoretical methods employed was responsible for the discrepancy between the transition-state structures predicted by theory and that indicated by the qualitative estimate of the experimental KIEs for the reaction in DMSO. It can thus be concluded that the transition state is reactant like, as was predicted by the theoretical calculations.

The chlorine leaving group, the nucleophile carbon and 2º α-D_2 KIEs were determined for the S_N2 reaction between some *para*-substituted benzyl chlorides and cyanide ion in THF. The interpretation of the KIEs in combination with theoretical calculations suggested that the transition states for these reactions were reactant like. According to the theoretical methods and the observed KIEs, the amount of bond fission to the cleaving group in the transition state decreases with the electron-withdrawing ability of the substituent. Moreover, the calculations indicate that the chlorine KIEs can be used as probes of the substituent effect on the C_α-Cl bond if bond fission is not too advanced in the transition state. The NC-Cα bond, on the other hand, did not appear to be very sensitive to the substituent. Theory predicted that there should be a larger amount of bond formation to the nucleophile in the transition state in the presence of an electron-withdrawing substituent, but this was not reflected in the observed KIEs. The results from the calculations concerning the nucleophile KIE were much less conclusive than those for the chlorine KIEs. According to the calculations, a clearly inverse KIE would be expected, even for the reactant-like transition structure predicted for the reaction investigated. Thus, the relation between the transition-state structure and the nucleophile KIE clearly needs to be investigated further.

5 Ion Association by Means of Precision Conductometry

Conductometry is the study of matter's ability to conduct electric current. In the case of liquids the charge carriers, or electrolytes, are ions. If the ions have high mobility the movement of charge will be extensive producing a large current, i.e. good conductivity is achieved. When two ions of the opposite charge come together and form an ion pair, the overall conductivity will decrease as these two charge carriers form a new uncharged entity, which is unable to contribute to the current. Likewise, the formation of higher aggregates, such as triple ions, which partially hamper charge transport, will also affect conductivity.

5.1 Principles of Precision Conductometry

When dealing with solid leads the ability to conduct current is usually given in terms of the resistance, R. The electric current, I, is inversely proportional to the resistance according to Ohm's law, Eq. (5.1), where V is the potential difference. In the study of liquids, the medium's conductivity, κ, is the favoured entity. The conductivity is, as can be seen in Eq. (5.2), the reciprocal of the resistance, thus being directly dependent on the electric current.

$$R = V/I \qquad \text{(Ohm's law)} \qquad (5.1)$$

$$\kappa = K_{cell}/R \qquad (5.2)$$

The cell constant, K_{cell}, is dependent on the dimensions of the conductivity cell used for the measurements. However, κ cannot be deduced directly from the resistance of an investigated solution, even if the cell's dimensions are known, as the division of current through the cell is highly complex. In practice, the cell is calibrated with a solution of well-known conductivity and the value of K_{cell} is then used to calculate the conductivity for the test solution from the measured resistance.

Naturally, the overall conductivity of a solution is dependent on the amount of charge carriers. Therefore, a better way to evaluate conductivity is by considering the molar conductivity, Λ_m, given by Eq. (5.3), in which c denotes the concentration of the electrolyte.

$$\Lambda_m = \kappa / c \qquad (5.3)$$

$$\Lambda = \Lambda_0 - k\, c^{1/2} \qquad \text{(Kohlrausch's law)} \qquad (5.4)$$

When dealing with 1:1 electrolytes the molar conductivity is the same as the equivalent conductivity, Λ. Judging by Eq. (5.3) conductivity seems to be directly dependent on electrolyte concentration in a straightforward manner. In reality, conductivity is dependent on the concentration in a more complex manner.

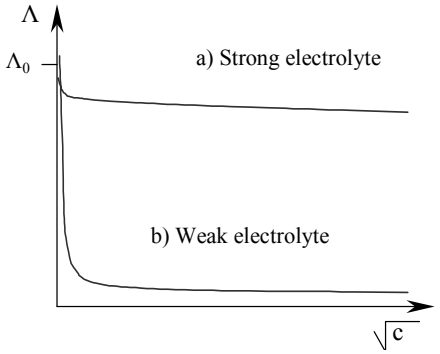

Figure 5.1 A schematic illustration of the concentration dependence for the conductance of a) a strong electrolyte, b) a weak electrolyte.

At very low concentrations, the solvated ions interact only with the solvent itself, i.e. the solution can be considered to be ideal. As the concentration increases the electrostatic interaction between the ions will become significant and cause ion mobility to decrease. For fully dissociated electrolytes, so-called strong electrolytes, conductivity is often successfully described by Eq. (5.4), where k is a constant primarily dependent on the stoichiometry of the electrolyte. Extrapolation to infinite concentration gives the equivalent conductivity at infinite dilution, Λ_0, which, for highly diluted solutions, can be used as an approximation of the equivalent conductivity, Λ. As can be seen in Figure 5.1, the behaviour of a weak, i.e. not fully dissociated, electrolyte is quite different. The decrease in conductivity due to association is drastic at low concentrations but levels out as the concentration increases. The degree of dissociation, α, of the electrolyte at a certain concentration can, as a first approximation, be calculated according to Eq. (5.5).

$$\alpha = \Lambda/\Lambda_0 \qquad (5.5)$$

In aqueous solution, potassium chloride will behave as a strong electrolyte, whereas acetic acid will act as a weak one. Additionally, the behaviour of an electrolyte also depends on the solvent used.

Let us now consider how ion pairing and triple-ion formation affect conductivity. The formation of ion pairs decreases the amount of charged entities and decrease more pronounced than that expected for a well-behaved strong electrolyte ensues. Figure 5.2a shows how ion pairing becomes more extensive with increased ion concentration.

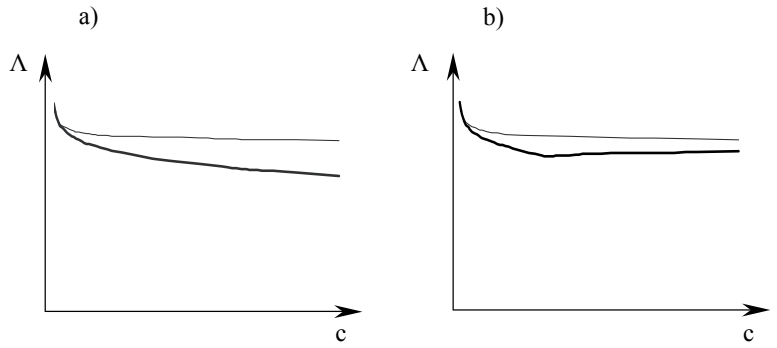

Figure 5.2 Influence on conductivity of a) ion pairing and b) ion pairing together with triple-ion formation. The thin line represents a fully dissociated electrolyte.

If further aggregation takes place and triple ions form, a slight increase in conductivity will follow,[57] see Figure 5.2b. As charged entities, triple ions contribute to conductivity but always to a lesser extent than single ions, which have more charge per unit volume. Once again, the observed behaviour of an electrolyte in solution is dependent on the combination of ions and solvent and not only the identity of the solute in question.

In order to determine the conductivity of a solution, the resistance is measured. A typical conductometry bridge is illustrated in Figure 5.3. The cell containing the electrolyte solution is placed in one branch of the circuit and the remaining resistances are balanced so that $R_2/R_1 = R_4/R_3$, at which point the galvanometer shows no deflection.

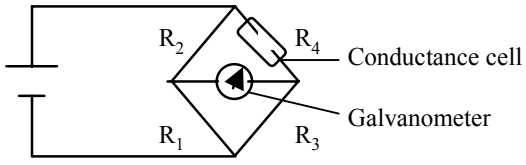

Figure 5.3 A basic circuit for a direct current bridge used for the measurement of electrolytic conductivity.

In order to avoid polarization of the electrolyte solution, the use of alternating (a.c.) current[58] has to a great extent replaced measurements with direct current. However, the principle of balancing the circuit with the electrolyte solution against circuits with known properties is the same. When a.c. is used the potential is balanced with regard to both phase and amplitude so that the impedance is in balance. The conductivity of the solution, $\kappa_{solution}$, calculated from the resistance of the solution, must be corrected for the conductivity of the solvent itself according to Eq. (5.6).

$$\kappa_{solute} = \kappa_{solution} - \kappa_{solvent} \qquad (5.6)$$

The lower concentration limit for precision conductometry is largely determined by the conductivity of the solvent, $\kappa_{solvent}$, which should be less than a few per cent of the conductivity originating from the solute. Concentrations down to 0.1–0.01 mM are applicable for most solvents.

At higher concentrations, sometimes already at 1 mM, inter-ionic influences will begin to reduce the conductivity more profoundly than Eq. (5.4) states. First, there is *the relaxation effect,* which has proven to be mathematically challenging.[59] The relaxation effect is envisioned most easily by considering the surroundings of a single ion in solution. At equilibrium, all ions will have a spherical "entourage" of oppositely charged ions. When the electric potential is applied, the ion moves from its central position leaving the centre of opposite charges behind. The consequence is an electrostatic field that exercises a force in the direction opposite to the applied potential until rearrangement, or relaxation, of the entourage has taken place. Extrapolation of the measured conductivity to infinite field frequency corrects the effect to some extent as the asymmetry of the surrounding ions is eliminated at higher frequencies. Secondly, *the electrophoretic effect* comes into play when the amount of electrolytes increases. As ions migrate in an electric field, they will encounter other migrating ions wrapped in their solvation shells. Collisions with ions moving in the opposite direction hamper mobility. Mathematically this effect has been treated by distribution functions for the electrolytes in accordance with Boltzmann.[59]

The temperature of the electrolyte solution also affects its conductivity. Increased temperature, unlike solids, leads to increased conductivity. With higher temperature follows lower viscosity, which in turn facilitates ion transport. Two different strategies are available to the experimentalist: either the temperature must be carefully controlled or the influence of temperature on the measured resistances must be corrected for. Immersing the cell in a tempered bath is however not as trivial as it might seem, as the presence of a liquid outside the cell can influence the measurements.[58,60]

5.1.1 Experimental Procedure (Paper IV)

The equipment used for the conductivity determinations presented in Paper IV consisted of an electrolytic conductivity bridge (4666 Leeds & Northrup) together with a Draggett-Bair-Kraus conductance cell[61] equipped with platinum-black-coated electrodes, see Figure 5.4. The cell was calibrated using an aqueous solution of potassium chloride.[62] Prior to each experiment, the conductivity of the solvent itself was determined before any electrolyte was added. The tetrabutylammonium cyanide was introduced in the form of a standard solution prepared by weight, corrected to vacuo. A calibrated automatic (10 or 20 mL) burette accurate to three decimal places was used to add the electrolyte solution. The temperature of the electrolyte solution in the cell was not controlled. Instead, it was closely monitored (± 0.005 ºC). For each experiment a temperature coefficient, spanning the experimental interval of 20–25 ºC, was determined at the highest electrolyte concentration. All measured resistances were corrected to 25 ºC. The resistance was measured for each concentration at three frequencies (2.00, 2.85 and 5.00 kHz). The resulting conductances served as the basis for extrapolation to infinite frequency.

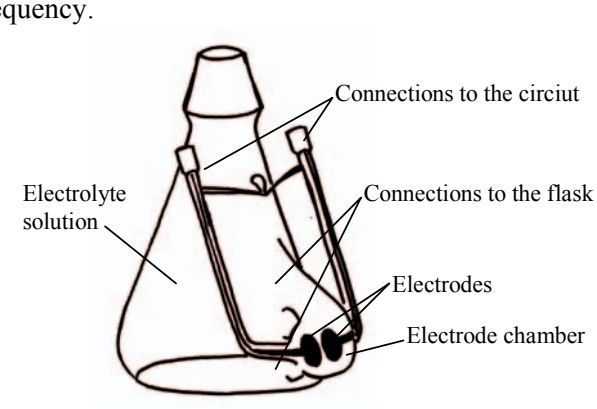

Figure 5.4 The conductance cell of Draggett, Bair and Kraus.

5.1.2 Data Interpretation

The concentration dependence of the conductivity data was interpreted by means of the Fuoss, Hsia, Fernandez-Prini (FHFP) equation,[63-65] see Eq. (5.7).

$$\Lambda = \Lambda_0 - S(c_i\alpha)^{1/2} + Ec_i\alpha\lg(c_i\alpha) + J_1c_i\alpha - J_2c_i\alpha^{3/2} - K_pc_i\alpha\gamma^2\Lambda \quad (5.7)$$

$$A^+ + B^- \rightleftharpoons AB \quad (5.8)$$

$$K_p = (1 - \alpha)/(c\gamma^2\alpha^2) \quad (5.9)$$

In the FHFP equation c_i denotes the concentration of free ions, α the degree of dissociation and K_p is the association constant for ion-pair formation (5.8) according to Eq. (5.9). S and E are constants depending on the dielectric constant (ε), viscosity (η) and temperature (T) of the solvent. The constants J_1 and J_2 depend on the same variables as S and E, but also on the critical distance between ions defined as ion pairs, q. In Paper IV the critical distance was set to the Bjerrum radius[66], see Eq. (5.10) where z is the ion charge, e represents the elementary charge and k_B is Boltzmann's constant. According to Bjerrum's theory for ion association, ions whose centres of charge are within this distance are considered ion pairs. At this distance or closer, electrostatic attraction exceeds the thermal energy of the ions and they form a distinct kinetic entity: the ion pair. The mean ionic activity constant, γ, is calculated according to the Debye-Hückel relation, Eq. (5.11) where A and B are constants dependent on ε and T.

$$q = |z_1 z_2| e^2/(2\varepsilon k_B T) \qquad (5.10)$$

$$\lg \gamma = A(c\alpha)^{1/2}/(1 + qB(c\alpha)^{1/2}) \qquad (5.11)$$

The equilibrium constant of ion-pair formation and the equivalent conductivity at infinite dilution were determined by an iterative procedure. This was based on the FHFP equation, rearranged to give the linear function presented in Figure 5.5, in combination with Eq. (5.11) and the law of mass action for the ion-pair equilibrium. The determined molar conductivities served as input data.

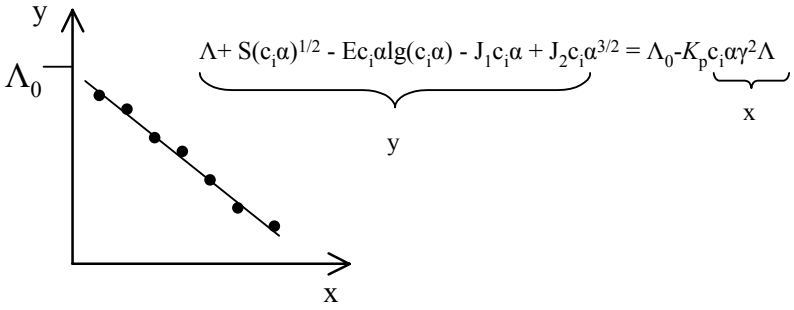

Figure 5.5 Linear arrangement of the FHFP equation used for the iterative determination of Λ_0 and K_p.

Generally, the formation of ion pairs is favoured by solvents of low polarity,[64] as is triple-ion formation.[57] Terms including equilibrium constants for triple ions can be added to Eq. (5.7) and the iterative process can be performed in analogy to the search for K_p and Λ_0. In theory, triple ions for univalent electrolytes can be expected at concentrations higher than the so-

called critical concentration limit, c_0, which is calculated according to Eq. (5.12).[67]

$$c_0 = 3.2 \cdot 10^{-7} \times \varepsilon^3 \qquad (5.12)$$

5.2 Ion Association of Tetrabutylammonium Cyanide in Water, DMSO and THF (Paper IV)

The study presented in Paper IV concerns the aggregation status and transport properties of tetrabutylammonium cyanide (Bu_4NCN) in water, DMSO and THF at 25 ºC. The Bu_4NCN concentrations employed and the dielectric constants of the investigated solvents are compiled in Table X together with the equilibrium constants found for ion-pair formation and the limiting molar conductivities.

Table 4. *The equilibrium constants for ion-pair formation and the limiting molar conductivities for tetrabutylammonium cyanide in water, DMSO and THF at 25 ºC, together with the dielectric constant for the solvents investigated and the electrolyte concentrations employed for the respective measurement series.*

Solvent	ε	Series	Concentration range (mM)	K_p	Λ_0 ($cm^2\Omega^{-1}mol^{-1}$)
H_2O	78.30[a]	1	0.143 – 0.359	196 ± 10[c]	115.6 ± 0.25[c]
”		2	0.657 – 5.663	–	–
DMSO	46.68[b]	3	1.022 – 13.00	1.98 ± 0.19	34.59 ± 0.03
THF	7.58[b]	4	0.002 – 0.031	$(59.6 \pm 0.6) \times 10^3$	10.71 ± 0.03
”		5	0.030 – 0.354	–	–
”		6	0.019 – 0.137	$(58.4 \pm 3.1) \times 10^3$	9.81 ± 0.23
”		7	0.569 – 11.26	–	–
”		8	10.48 – 11.97	–	–

[a] Reference 68. [b] Reference 69. [c] Standard deviation.

Tetrabutylammonium Cyanide in Water

The K_p value of 196, which corresponds to the slope of the straight line in the FHFP x-y plot in Figure 5.6, indicates significant ion-pair formation. Most univalent electrolytes are expected to be almost completely dissociated in aqueous solution as water is a strongly solvating medium for charged species. This result is also surprising in the light of an estimate of the minimum distance possible between the charges of the $Bu_4N^+CN^-$ ion pair, based on the radius of the Bu_4N^+ ion and half a CN triple bond.[70] As this estimate of 5.52 Å exceeds 3.58 Å, which is the critical distance for an ion pair according to Bjerrum's theory, it would be unlikely to find Bu_4NCN in

the form of ion pairs. This type of unexpected behaviour has previously been observed for quaternary ammonium salts in protic solvents, for which other causes of aggregation, such as hydrophobic interactions, have been considered apart from electrostatic interactions.[71]

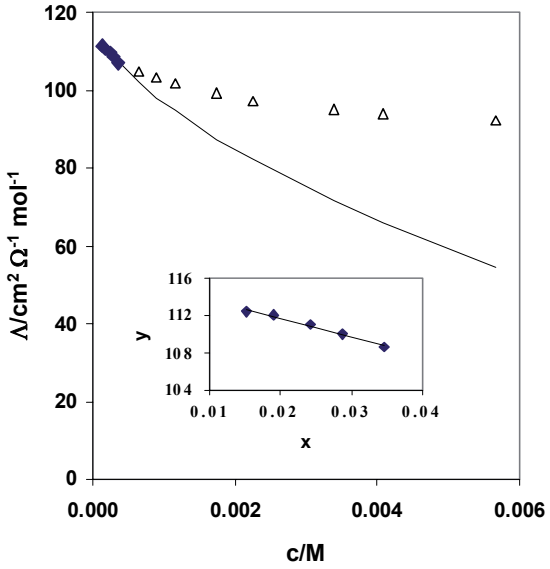

Figure 5.6 The molar conductivity of Bu_4NCN in H_2O at 25 ºC for series 1 and 2 together with the molar conductivity according to the FHFP equation extrapolated from the lower to the higher concentration range, shown as a solid line. The inserted plot is the corresponding FHFP x-y plot.

The intercept of the FHFP x-y plot presented in Figure 5.6 corresponds to a limiting molar conductivity of Bu_4NCN of 115.6 $cm^2\Omega^{-1}mol^{-1}$. In combination with the limiting molar conductivity of the Bu_4N^+ ion[68] of 19.4 $cm^2\Omega^{-1}mol^{-1}$ this value yields a limiting molar conductivity for the cyanide ion of 96 $cm^2\Omega^{-1}mol^{-1}$. This is very high as the value is greatly exceeded only by the limiting molar conductivity for the oxonium and hydroxide ions.

As can be seen in Figure 5.6, above approximately 0.4 mM the experimental molar conductivity of Bu_4NCN in H_2O deviates positively from that predicted by the FHFP equation. The reason for this remains to be elucidated, but it is phenomenologically similar to the effect of triple-ion formation in solvents of low polarity such as THF.

Tetrabutylammonium Cyanide in DMSO

Despite the lower dielectric constant of DMSO than water, see Table X, the extent of ion pairing of Bu_4NCN is noticeably less in DMSO than in aqueous solution. The low K_p value of 1.98 is reflected by the almost horizontal line of the FHFP x-y plot depicted in Figure 5.7.

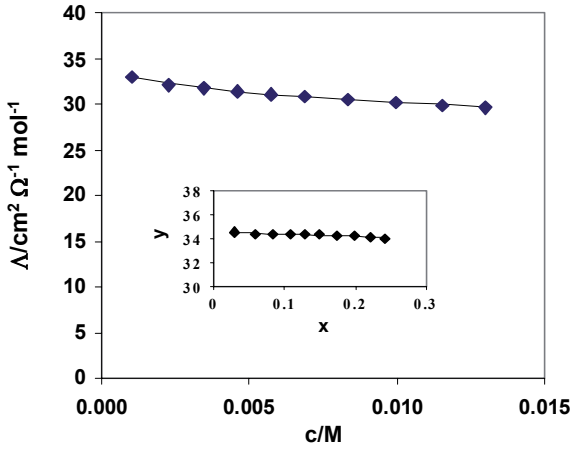

Figure 5.7 The molar conductivity of Bu_4NCN in DMSO at 25 ºC for series 3, together with the molar conductivity according to the FHFP equation, shown as a solid line. The inserted plot is the corresponding FHFP x-y plot.

Tetrabutylammonium Cyanide in THF

In solvents with low dielectric constants, the observation of ion pairs is restricted to a narrow concentration window due to significant formation of higher aggregates, even at modest concentrations. In THF the critical concentration limit for the formation of triple ions according to Eq. (5.12) is 1.4×10^{-4} M. Thus, in order to determine K_p and Λ_0 the low concentration range from 2 to 31 μM was investigated, see Figure 5.8.

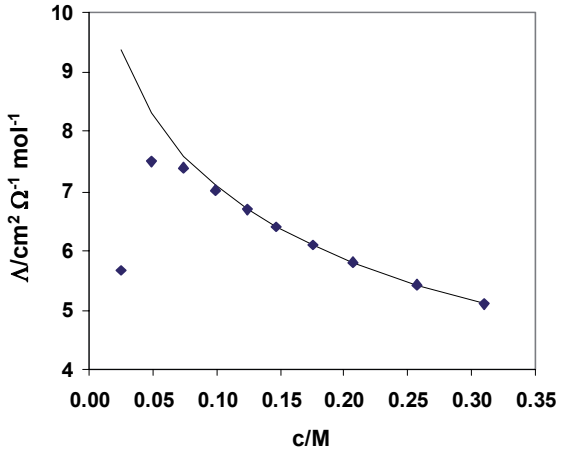

Figure 5.8 The molar conductivity of Bu_4NCN in THF at 25 ºC for series 4 together with the molar conductivity according to the FHFP equation fitted to the six points of the highest concentration, shown as a solid line.

At concentrations below 10 μM the measured conductivites were significantly less than those that could be expected from the rest of the

experimental series. The probable cause of this is adsorption of the electrolytes to the electrode surfaces, which has been shown to occur.[68] In any case, this behaviour implies that the lower concentration limit of the equipment utilized had been reached. Usually, this limit is set by the conductivity of the solvent itself, but in this case the conductivity of the THF was so low that the measured conductivities for Bu_4NCN did not even need to be corrected. The conductivities measured above 10 μM in series 4 resulted in a value of Λ_0 of 10.71 $cm^2\Omega^{-1}mol^{-1}$ and of K_p of 59.6×10^{-3}, the latter of which indicates substantial ion-pair formation. These values are in excellent agreement with the Λ_0 of 9.81 $cm^2\Omega^{-1}mol^{-1}$ and K_p of 58.4×10^{-3} that resulted from series 6.

Figure 5.9 shows the compiled molar conductivities of series 5–8. The conductance curve displays a minimum, which implies that the experimental points in the higher concentration range exceed the conductivity predicted by FHFP theory. This type of behaviour has been observed previously and explained in terms of triple-ion formation.[72]

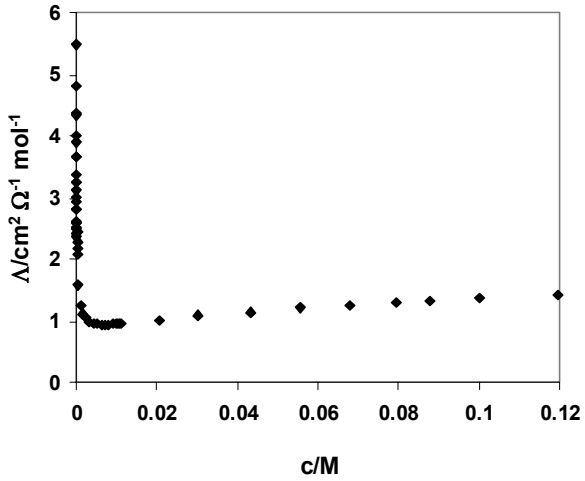

Figure 5.9 The molar conductivity of Bu_4NCN in THF at 25 ºC for series 5–8.

The introduction of a triple-ion association constant in order to achieve better agreement between the experimental data and theory has been performed successfully in studies of sodium iodide in 1-octanol and tetrabutylammonium picrate in chlorobenzene.[73,74] Unfortunately, such a qualitative assessment of the amount of triple-ion formation cannot be undertaken in this study as the data in the concentration range from 0.014 mM to 0.02 mM are insufficient.

The Aggregation Status of Bu_4NCN in Water, DMSO and THF

The aggregation status of Bu_4NCN was found to be very different in the investigated solvents. The tendency for ion-pair formation in DMSO is very slight whereas it is significant and very strong in water and THF, respectively. In Figure 5.10 the degree of dissociation, α, for Bu_4NCN in water, DMSO and THF is presented as a function of the concentration. It is evident that in DMSO the Bu_4NCN is almost exclusively in the form of dissociated ions, even at a concentration of 0.8 mM. At the same concentration in water, the degree of dissociation has decreased to 0.88 due to the formation of ion pairs. The degree of dissociation of Bu_4NCN in THF is only presented up to 0.2 mM as the amount of higher aggregation is significant already at this concentration.

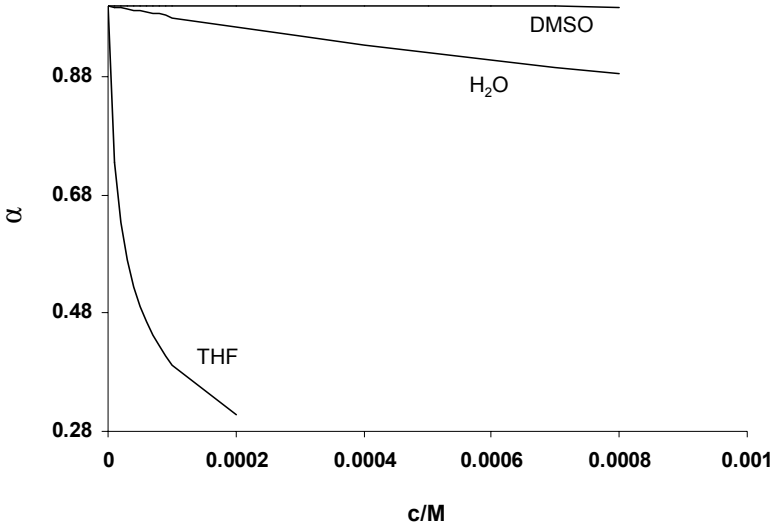

Figure 5.10 The degree of dissociation, α, of Bu_4NCN in DMSO, H_2O and THF.

As the conductance theory is limited to the study of relatively low concentrations it is not possible to gain any quantitative information on the aggregation status at higher concentrations than those presented in Figure 5.10. However, a qualitative estimate indicates that the degree of dissociation of Bu_4NCN in DMSO remains relatively high, i.e. >90%, even at a concentration of 0.1 M. The high degree of aggregation of Bu_4NCN found in THF at modest concentrations will be maintained with increasing concentration. The degree of dissociation expected in the concentration range of 0.02–0.1 M is probably less than 0.05.

5.3 Implications on Kinetic Isotope Effect Studies

The most important conclusion in connection with the use of KIEs is that the aggregation status of Bu_4NCN is very different in the two solvents THF and DMSO. The impact on the force constant of the CN triple bond, upon for example ion pairing, could be investigated by means of theoretical methods. Thus, the influence of aggregation on the kinetic isotope effect can be assessed in greater detail.

5.4 Conclusions and Outlook

In contrast to what is generally expected for univalent salts, the tendency towards ion pairing in water was found to be significant, with a value of K_p of 196. Moreover, the molar conductivity of Bu_4NCN was found to exceed that predicted by the FHFP theory in a manner that phenomenologically resembled the formation of higher aggregates. The limiting molar conductivity of the cyanide ion in water was determined to be 96 $cm^2\Omega^{-1}mol^{-1}$, which is relatively high. In order to verify this value, further measurements of the cyanide ion in combination with other cations than the tetrabutylammonium ion are required.

The value of K_p of 1.98 determined for Bu_4NCN in DMSO implies that there is a high degree of dissociation.

The conductivity data for Bu_4NCN in THF indicate that there is a high tendency for ion-pair formation, $K_p = 58.4\times10^3$, and higher aggregates are formed even at low concentrations. If an equilibrium constant for the formation of triple ions is to be determined, the concentration interval of 0.014–0.02 mM must be further investigated.

6 Gaining Insight into the Mechanism of Monoamine Oxidase through Nitrogen Kinetic Isotope Effects

6.1 Monoamine Oxidase

Monoamine oxidases (MAOs) are flavin-dependent enzymes that catalyse the oxidation of many primary, secondary and some tertiary amines to their corresponding protonated imines. These enzymes are bound to the outer membrane of the mitochondria and can be found in many eukaryotic organisms such as mammals, amphibians, fish, birds and some fungi.[75] As can be seen in Figure 6.1, which illustrates the MAO-catalysed oxidation of benzyl amine, the protonated imine is subsequently hydrolysed to the corresponding carbonyl compound non-enzymatically, and the MAO is regenerated to its active form by molecular oxygen, which in turn is reduced to hydrogen peroxide.

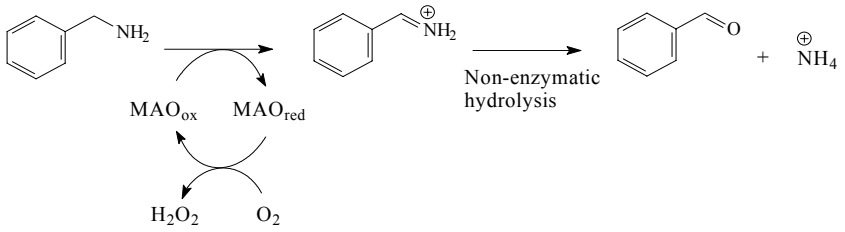

Figure 6.1 The MAO-catalysed oxidation of benzylamine and the regeneration of the enzyme to its active form. MAO_{ox} and MAO_{red} denote the oxidized and the reduced states of the enzyme, respectively.

The FAD (flavin adenine dinucleotide) co-factor essential for catalysis,[76] is covalently bound to the enzyme via a thioether linkage between an active site cysteine residue and the 8α-methyl group of the isoalloxazine ring, see Figure 6.2.

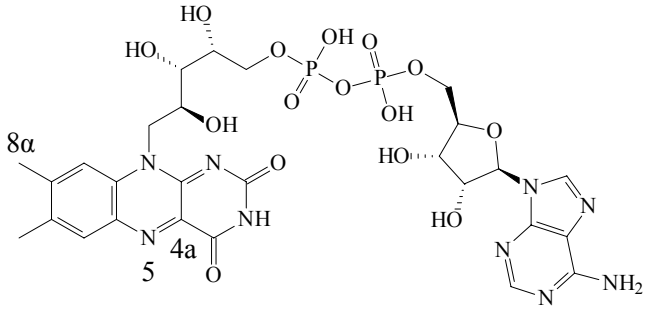

Figure 6.2 The flavin adenine dinucleotide (FAD) and partial numbering of the isoalloxazine ring system.

In mammals, MAOs exists in two different forms,[77] or isozymes, 71% of the amino acid sequences being identical.[78] The isozymes A and B (MAO A and MAO B) differ partly in their substrate and inhibitor specificities, as can be seen in Figure 6.3. MAO B substrates are generally smaller in size and have a more hydrophobic character than MAO A substrates.

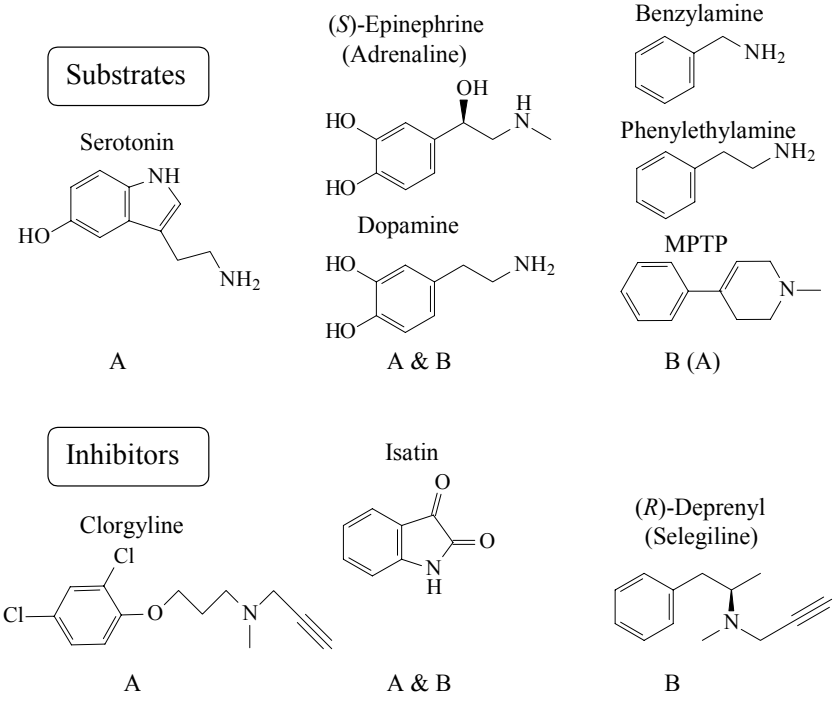

Figure 6.3 A small selection of substrates and inhibitors of MAO A and B. Notation within brackets implies compatibility but to a lesser extent. MPTP denotes 1-methyl-4-phenyl-1,2,3,6-tetrahydropyridine.

In their capacity as amine oxidation catalysts, monoamine oxidases serve as detoxifiers in peripheral organs and as neurotransmitter regulators in the

brain. Being of such vital physiological importance it is hardly surprising to find ample examples of MAOs in connection with medical research.[79,80] Two of the most well known examples of MAO inhibitors in applied medicine are the use of MAO A inhibitors as antidepressants and the combination of L-DOPA and MAO B inhibitors as a symptom alleviator in Parkinson's disease.[79] Other neurodegenerative diseases such as Alzheimer's, Huntington's and amyotrophic lateral sclerosis (ALS) are also thought to be connected with MAOs.[79] Examples of other research areas within which monoamine oxidases are of importance are tumour malignancy,[81] ageing,[82] cell growth,[83] personality traits[84] and physiological responses to tobacco smoke and coffee.[85,86]

Most human tissues express both MAO A and B but the exact ratio of the two isozymes differs greatly from one organ to another. Inhibitors intended for use as therapeutic agents must thus not only be efficient but also highly selective between the two isozymes of MAO as well as other enzymes in order to avoid side effects from therapy.

6.1.1 The Quest for the Mechanism

Many different approaches have been used to gain insight into how monoamine oxidase pursues catalysis, including steady-state and stopped-flow kinetics with accompanying hydrogen KIEs, site-directed mutagenesis, mechanism-based inhibitors, detection of reaction intermediates and structure-activity relationships of substrates and inhibitors. However, the mechanism by which MAOs catalyse amine oxidation still remains to be unambiguously established.

It is often assumed that MAO A and B act by the same mechanism, and that the differences in substrate and inhibitor specificities stem from structural features of the active sites of the respective isozyme. The overall pathway for MAO catalysis, which is presented in Figure 6.4, exhibits dependence on isozyme as well as on substrate.[87,88] For example, oxidation of benzylamine by MAO B proceeds via the lower route in Figure 6.4, where reoxidation of the enzyme takes place before the product is released. On the other hand, oxidation of phenylethylamine by the same isozyme follows the upper path in the scheme, which means that enzyme reoxidation succeeds product release.

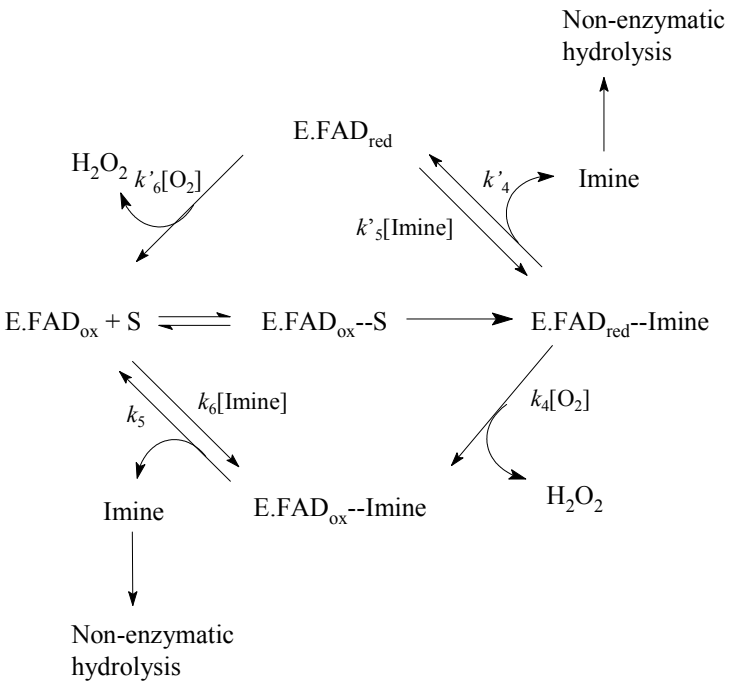

Figure 6.4 Reaction pathways for MAO catalysis and regeneration.

Further information on MAO A and B catalysis of the commonly used substrates benzylamine and phenylethylamine is presented in Table 1. One clearly noticeable difference between the A and B isozymes is that in their $K_{M(O2)}$ values, of 6 and 250 μM, respectively. This means that MAO B can never reach more than half the maximal velocity predicted by $K_{M(substrate)}$ since approximately 250 μM is the concentration of O_2 in aqueous air-saturated solutions. Much more concordant behaviour, with neglect of phenylethylamine and MAO B, is seen when considering the magnitudes of the KIEs for the turnover ($^Dk_{cat}$) and flavin reduction ($^Dk_{red}$), which imply that the cleavage of the α-hydrogen carbon bond is likely to be, either fully or to a large degree, the rate-limiting step of catalysis. Likewise, the similar rates of enzyme reduction and catalytic turnover imply that the rate limitation in the catalytic turnover is largely due to enzyme reduction. The quantitative structure-activity relationship of k_{red} and k_{cat} (MAO A with *para*-substituted benzylamines) is in accord with proton abstraction as the mode of hydrogen-carbon bond cleavage. It has further been proposed that MAO B catalysis also proceeds via proton abstraction, and that the lack of electronic effects on the catalytic rate of MAO B stems from steric constraints on the substrate in the active site preventing charge delocalization to the phenyl ring.[89]

The only experimental work elucidating contributions from tunnelling in MAO catalysis has been reported on bovine liver MAO B with *para*-

methoxybenzylamine as the substrate.[90] The results confirmed tunnelling and thus it is likely that tunnelling will also be observed in human MAO B catalysis. A great deal of similarity between MAOs in mammals is to be expected, but it may not be possible to extrapolate experimental results concerning MAOs from one species to another.[91]

Table 5. *A selection of kinetic parameters regarding MAO A and B catalysis of benzylamine and phenylethylamine together with hydrogen KIEs, the results of some structure-activity relationship studies and the inferred identification of the rate-limiting step of catalysis.*

MAO	A		B	
Substrate	Benzylamine	Phenylethylamine	Benzylamine	Phenylethylamine
Enzyme source	Human liver[a]	Human liver[b]	Bovine liver[c] Human liver[d]	Bovine liver[e]
K_M (μM)	1040 ± 150	1250 ± 69	500 ± 60 500 ± 100	500
k_{cat} (min^{-1})	2.54 ± 0.08	64 ± 1.2	640 ± 56 600 ± 110	1250
$K_{M(O_2)}$ (μM)	~ 6		~ 250	
$^{D}k_{cat}$	11.5 ± 0.6	8.5 ± 0.3	8.2 ± 0.9 4.7 ± 1.0	~1
$^{D}k_{red}$[f]	9.3 ± 1.2	7.3 ± 0.7	10.1 ± 0.1	3
$^{D}(k_{cat}/K_M)$	12.1 ± 2.3	9.6 ± 1.3	5.2 ± 0.4 4.5 ± 1.4	
QSAR[g] *p*-subst. (k_{red}&k_{cat})	ρ = 2.0[h]	Negative correlation with V_w[i]	Negative correlation with E_s[j]	
RLS[k]	α C –H cleavage	α C –H cleavage	α C –H cleavage	Reoxidation of the reduced enzyme

[a] 11 ºC, reference 89. [b] 11 ºC, reference 92. [c] 25 ºC, reference 93. [d] 25 ºC, reference 94. [e] reference 95. [f] Rate of flavin reduction determined by anaerobic stopped flow measurements. [g] Quantitative structure-activity relationship of *para*-substituted analogues. [h] Hammett ρ-value. [i] van der Waals volume. [j] Taft parameter for steric influence. [k] Rate-limiting step of catalysis.

The Three-Dimensional Structure of Human MAO

For a long time mechanism research on MAOs had to be performed without knowledge of the three-dimensional structure of the enzyme. However, the structures of both isozymes of human liver MAO and rat liver MAO A were recently elucidated by X-ray crystallography.[96-99] The overall chain folds of the two isozymes of human MAO resemble one another in many ways. However, the A isozyme crystallizes as a monomer, whereas MAO B forms dimers with a contact area corresponding to 15% of the monomer surface. To date, no interaction between the active sites of the dimers has been observed. The C-terminal helix, see Figure 6.5, which is inserted into the mitochondrial membrane not only functions as an attachment, but is also important for the stability of the enzyme.[100] The entrance to the active cavity is situated close to the membrane surface and, in the case of MAO B, on the opposite side to the dimer contact area.

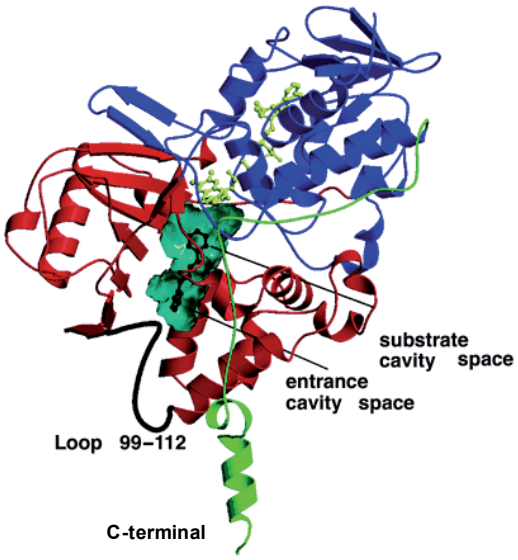

Figure 6.5 The overall three-dimensional structure of a monomer unit of human MAO B in complex with 1,4-diphenyl-2-butene. The inhibitor and FAD cofactor are represented by ball-and-stick representations in black and grey respectively. Reproduced with permission from reference 97.

The conformation of the loop formed by amino acids 210–216 differs distinctly between MAO A and B. It determines to a large extent the shape and size of the active site cavities of the two isozymes. The wide, but rather short, substrate cavity of MAO A is approximately 550 $Å^3$, while MAO B has a substrate cavity that is larger in overall size, 700 $Å^3$, but of a more elongated and narrow shape. Furthermore, the MAO B cavity is divided into two parts: the entrance and substrate cavities. The "gate" between them consists of isoleucine 199, which has to rotate out of its normal conformation in order to accommodate inhibitors that span both cavities.[101] The active sites

of MAO A and B are lined with aromatic and aliphatic amino-acid side chains creating a hydrophobic environment. The flavin cofactor, located at the end of the substrate cavity, exposes its *re* face* and is flanked by two tyrosine residues that form an aromatic cage, see Figure 6.6. The isoalloxazine ring is twisted to about 30º and N5 is hydrogen bound to a leucine via a water molecule.

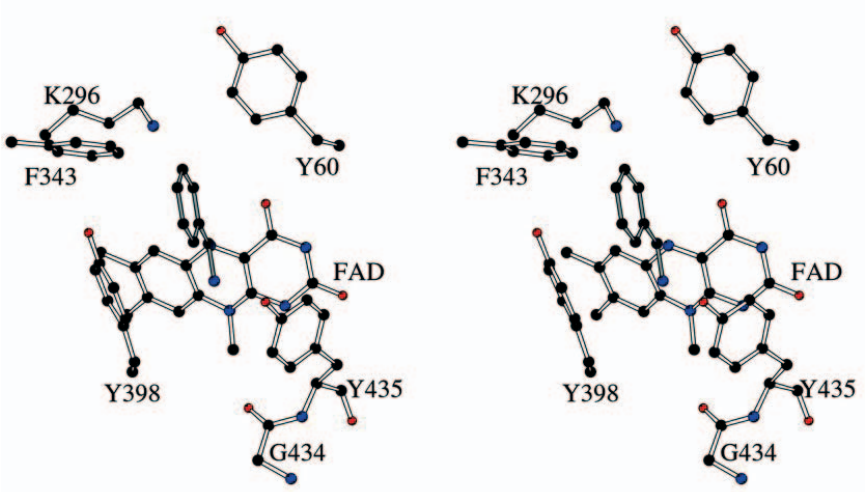

Figure 6.6 A stereoview of benzylamine modelled into the catalytic site of human MAO B. The aromatic cage consisting of two tyrosines (Y398 and Y435) is shown together with other amino-acid side chains of the active site. K, G and F denote lysine, glycine and phenylalanine, respectively. Reproduced with permission from reference 102.

Proposed Mechanisms

Several mechanisms have been proposed during the years, but attention is currently being devoted mainly to the aminium cation radical mechanism described by R. B. Silverman[103-105] and the polar nucleophilic mechanism as presented by D. E. Edmondson.[89]

The radical mechanism (Figure 6.7) is initiated by reversible, single-electron transfer from the unprotonated amine to the flavin producing a flavin radical and an aminium cation radical intermediate. The radical intermediate undergoes proton abstraction and further oxidation will then take place directly or via adduct formation. The initial electron transfer and proton abstraction may, according to a recent amendment by Silverman,[103,104] be concerted.

* With reference to the 4a carbon.

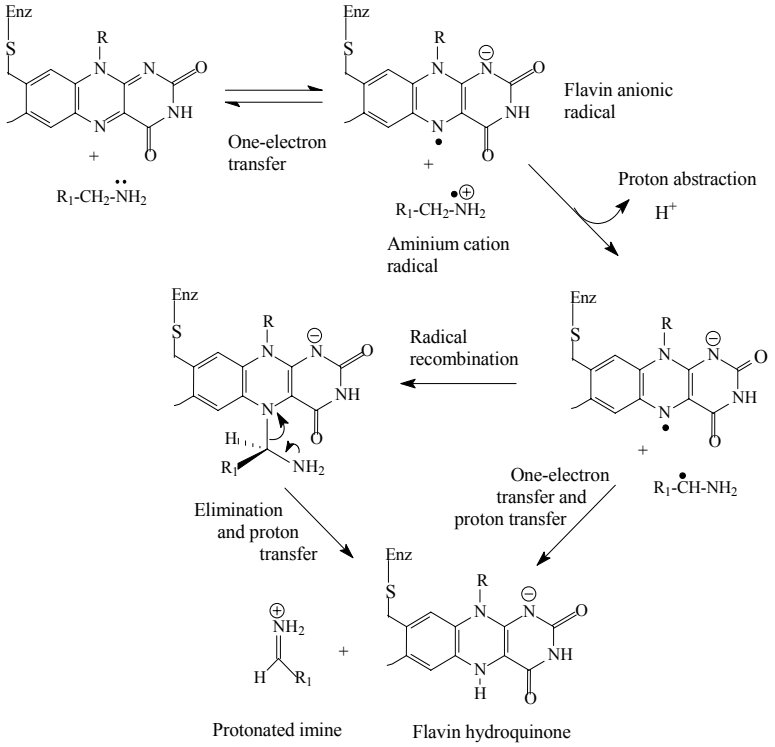

Figure 6.7 The aminium cation radical mechanism proposed by Silverman *et al.*[103-105] R, R_1 and Enz denote the ribityl chain leading to the dinucleotide moiety, an arbitrary alkyl/aryl group and the point of attachment to the enzyme, respectively.

The radical mechanism is based on the single-electron transfer commonly encountered in electrochemical oxidation of amines, and is in accordance with the results of several inhibitor studies performed by Silverman.[106] The regioselectivity found in the MAO B-catalysed oxidation of a tertiary amine is also consistent with a radical mechanism.[107] The identity of the active site radical is crucial for this mechanism. Spectroscopic evidence indicating the presence of a stable tyrosyl radical after reductive titration of human MAO A has been presented.[108] The evidence was in line with the tyrosyl radical being in rapid exchange with the flavin semiquinone. It has recently been shown that these results may be based on an artefact arising from the comparison between a covalent and a non-covalent flavin anionic radical.[109] The existence of a radical during catalysis has not been established by magnetic field effects on the reaction rate[110] or by spectroscopic evidence of a flavin radical.[93,111] However, the main difficulty associated with direct observations of reaction intermediates is that their turnover may be too rapid for any detectable amounts to build up. A further objection to the radical mechanism has been presented by Edmondson who stated that a ground-state flavin is unlikely to oxidize a primary amine via a one-electron step due to

their respective oxidation potentials.[89] It should also be noted that the identity of the base abstracting the proton from the aminium cation radical is unknown and that no plausible amino-acid candidate has been found bearing in mind the three-dimensional structure of the enzyme.

According to the polar nucleophilic mechanism proposed by Edmondson, the initial step is nucleophilic attack by the unprotonated amine on the flavin C4a, see Figure 6.8. The resulting C4a adduct then decomposes to form the reduced flavin and the protonated imine. Proton abstraction may be concerted with either adduct formation (right-hand route) or product formation (left-hand route).

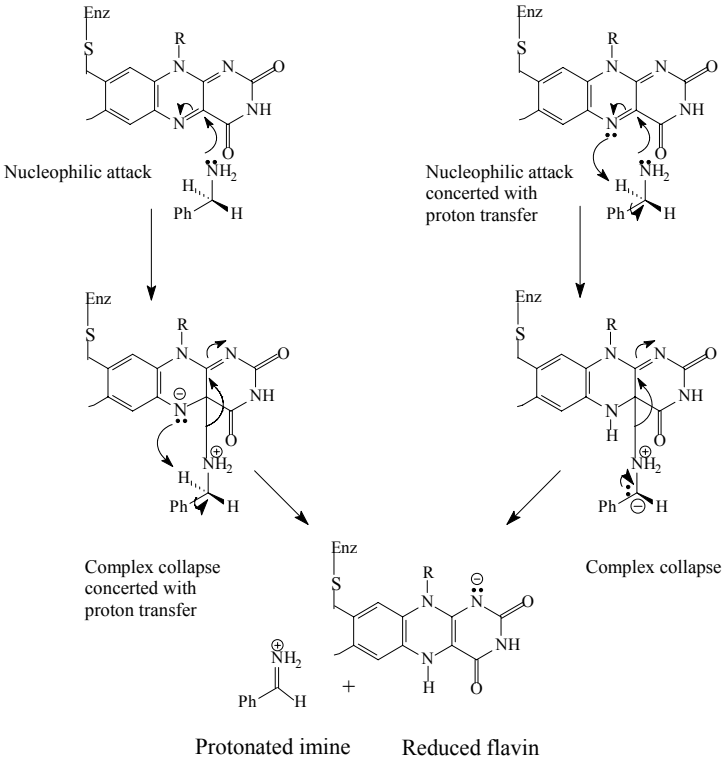

Figure 6.8 The polar nucleophilic mechanism as proposed by Edmondson *et al*.[88,89] R and Enz denote the ribityl chain leading to the dinucleotide moiety and the point of attachment to the enzyme, respectively.

The basicity of the flavin N5 is thought to increase under the influence of the incoming nucleophile/adduct formed, and the resulting structural arrangement will give the stereoselectivity observed in catalysis, which is abstraction of the *pro-(R)* proton.[112] Non-enzymatic model studies have shown the formation of a stable C4a adduct between a lumiflavin and benzyl amine[113] and that the rates of oxidation of some primary and secondary amines with a similar lumiflavin are correlated with amine nucleophilicity.[114]

Furthermore, Edmondson argues that the non-planar conformation observed for the enzyme-bound isoalloxazine ring system is likely to make adduct formation to N5 or C4a less constrained.[97] According to Edmondson the aromatic cage consisting of the two tyrosines may be vital for the alignment of the substrate. The aromatic cage would be expected to sufficiently stabilize an aminium cation radical through π-interactions to render it detectable by spectroscopy.[88] Recently performed semi-empirical calculations on the isoalloxazine ring system and some *para*-substituted benzylamines undergoing the polar nucleophilic mechanism support adduct formation as the rate-limiting step of the reaction and the result from the structure-activity relationship of MAO B.[115]

6.2 Nitrogen Kinetic Isotope Effect for the Deamination of Benzylamine by MAO B (Paper V)

The body of evidence, although ample, lacks the power of discrimination as both mechanisms are consistent with the observed KIEs and proton abstraction as the (fully or to a large degree) rate-limiting step. In the hope of obtaining discriminating evidence, the nitrogen KIE for the deamination of benzylamine by MAO B was determined.

The $^{15}(V/K)$, see Table 6, was determined under steady-state conditions with respect to substrate concentration. Competitive kinetics was applied and a chromatographic procedure in combination with isotope ratio mass spectrometry (IRMS) at natural abundance provided the fraction of reaction and isotopic ratio ($^{14}N/^{15}N$) of the substrate. (For further information on the experimental procedure see Section 7.1.)

As the determination of $^{15}(V/K)$ was performed at pH 7.5 and the enzyme acts on the unprotonated amine[92,116,117] the observed KIE must be corrected for the equilibrium isotope effect on deprotonation.[35] The value of $^{15}K_{eq}$ for phenylalanine[25] was used, as the value of EIE for benzylamine is likely to be very similar. The intrinsic KIE was thus estimated to be 0.9909.

If one considers the polar nucleophilic mechanism depicted in Figure 6.8, the left-hand alternative, with the complex collapse as the main rate-limiting step, does not seem plausible in the light of the Hammett ρ-value. In this step there is no build-up of formal charge, and unless the five-membered transition state is extremely asynchronous in its bond fission/formation it is difficult to envisage the substantial Hammett reaction constant ($\rho = 2.0$). The charge build-up on the benzylic carbon in the adduct formation according to the route on the right in Figure 6.8, would, on the other hand, constitute a feasible cause of a high ρ-value. Moreover, recent theoretical findings[115] support this alternative.

Table 6. *The value of $^{15}(V/K)$ for the deamination of Benzylamine by monoamine oxidase B in 50 mM HEPES buffer with Triton X-100 reduced (0.5%) at 25.0 °C* [a]

Experiment	Fraction of reaction (*f*)	R_f/R_0 [b]	$^{15}(V/K)$ [c]	Average
1	0.1852	1.001890	1.00935	
2	0.2584	1.001922	1.00647	
3	0.1330	1.000890	1.00627	
4	0.1372	1.001088	1.00742	
5	0.1776	1.000958	1.00492	
6	0.1786	1.001365	1.00698	
7[d]	0.1384	1.000891	1.00601	
8[d]	0.1893	1.001646	1.00790	
n = 8				**1.0069 ± 0.0005**[e]
The resulting KIE after correction for $^{15}K_{eq}$ [f]				**0.9909**

[a] The initial substrate concentration in these experiments was approximately 6 mM. In order to ensure full irreversibility of the reaction semicarbazide hydrochloride was added to the solution in order to act as an aldehyde trap. [b] R_f is the isotopic ratio of benzylamine at fraction of reaction, *f*. R_0 is the isotopic ratio at 0% conversion. [c] The isotope effect is calculated using the formula $^{15}(V/K) = \ln(1 - f)/[(1 - f)(R_f/R_0)]$. [d] Experiments carried out on a separate occasion with a different batch of enzyme. [e] Standard deviation of the mean. [f] The $^{15}K_{eq}$ value of 1.0163 for the deprotonation of phenylalanine was taken from reference 25 and 9.46 was used for the pK_a of benzylamine.

The observed nitrogen KIE would thus be a nucleophile KIE. Nitrogen KIEs of 0.97–1.03 have been observed,[35] and a computational study on incoming 1º nitrogen KIEs for nucleophilic attacks on sp^3 carbons has predicted that an inverse isotope effect would ensue when the bond order of the formed C-N bond is greater than 0.5 in the TS.[36] The observed inverse nitrogen KIE of about 1% could thus stem from a fairly advanced bond formation in the transition state between the incoming nucleophile and the C4a of the flavin. This would be reasonable as the basicity of the flavin N5 has to develop sufficiently in order to abstract the α-proton in a concerted manner.

How then, does the observed KIE correspond to the proposed radical mechanism? The proton transfer in Figure 6.7, which is known to contribute significantly to the rate of catalysis, does not induce any major change in bond order or geometry for the nitrogen atom. The same applies to the initial one-electron transfer which, due to its endothermic nature may also contribute to some degree to the overall rate. This two-step sequence is not likely to be accompanied by any major change in the force constant of the nitrogen bonds and will therefore not result in any significant KIE.

The situation is thus that the observed nitrogen KIE corresponds well with the polar nucleophilic mechanism, but it does not exclude the radical mechanism.

Let us assume that the observed nitrogen KIE results from the radical mechanism. What would then be expected? The two steps of interest are, as mentioned above, the initial single-electron transfer (SET) and the proton abstraction. The aminium cation radical produced in the SET oxidation would probably have a slightly pyramidal conformation as a consequence of hyperconjugative stabilization.[118] The nitrogen KIE expected from this step would probably be very small and possibly inverse based on the same reasoning that has been applied to central carbon KIEs for S_N1 reactions.[119] The observed central-atom KIEs of S_N1 reactions are much smaller than those of S_N2 reactions, although there is no bond formation to compensate for the bond fission. The rationale for this has been stated to be that hyperconjugation partially compensates for the loss of TS bond order due to ionization. Whereas the S_N1 central-atom KIEs are normal, the KIE for the radical formation may become inverse if the hyperconjugation were to overcompensate the change in electronic conditions as no bond is broken during single-electron transfer. Proton abstraction would probably also result in a very small nitrogen KIE. The change in geometry of the nitrogen atom will be from slightly pyramidal to more pyramidal as the radical is likely to be mostly delocalised over the phenyl ring. This can be seen as being close to the reverse process compared to the first step. Thus, the deviation of the isotopic rate ratio of the proton abstraction from unity is expected to be the reciprocal of the KIE for the first step. The observed nitrogen KIE will then be determined by the balance between the contributions to the overall rate by the two steps. The nitrogen KIE would then be sensitive to isotopic substitution of the α-protons as the proton abstraction would become yet more rate limiting than before. A nitrogen KIE originating from the polar nucleophilic mechanism, on the other hand, would be expected to be insensitive to isotopic substitution of the α-protons as: *i*) the contribution to the overall rate from the adduct formation step is likely to be close to its maximum without α-deuteration and *ii*) the nucleophilic attack and the proton abstraction are concerted.

The $^{15}(V/K)_D$ for the Deamination of Benzylamine by MAO B

The value of $^{15}(V/K)_D$ was determined according to the same procedure as described above, but with some minor alterations. In order to achieve at least the same fraction of reaction as for the $^{15}(V/K)$ experiments, the reaction time was extended in combination with an increased amount of added enzyme. The (1,1-$^2H_2$)benzylamine was synthesized by $LiAl^2H_4$ reduction of benzonitrile according to procedures previously used for the synthesis of MAO substrates.[90,120]

Unfortunately, $^{15}(V/K)_D$ has so far resisted determination twice. The first attempt probably failed due to too long a storage time before the IRMS analysis. Two new attempts were made to determine $^{15}(V/K)$ in order to

establish if any additional problems had arisen in the experimental set-up since the initial $^{15}(V/K)$ series. As these two values, see entries 7 and 8 in Table 2, were in agreement with the initial series, it was concluded that there was no additional source of error, apart from the extended storage time, and thus the second $^{15}(V/K)_D$ series was begun. In this case, failure was due to the enzyme, which showed low or no activity with either deuterated or undeuterated benzylamine. Others working with the same batch of enzyme encountered no difficulties and a second batch of enzyme did not improve the situation. In the end no plausible cause could be found for this behaviour, and the experimental work was temporarily suspended.

6.3 Conclusions and Outlook

The observed $^{15}(V/K)$ of 0.9909 is in accord with the polar nucleophilic mechanism as proposed by Edmondson, but it cannot be ruled out that such a modest KIE could result from the radical mechanism suggested by Silverman. As attempts to determine $^{15}(V/K)_D$ have failed so far, the possibility of distinguishing between the two mechanisms by means of multiple isotope effects still remains unexplored. However, if Silverman is correct in his recent amendment, i.e. that the proton transfer and the initial single-electron transfer may be concerted, then the multiple isotope effects would not provide any discrimination between the two proposed mechanisms.

On the other hand, if the determination of $^{15}(V/K)_D$ were to succeed and prove useful in the case of MAO B, continued nitrogen KIE studies on MAO A would be justified. The preferred substrate in such a study would be phenylethylamine as benzylamine oxidation by MAO A is too slow. In the light of the substantial Hammett ρ-value found for MAO A oxidation of *para*-substituted phenylethylamines, inclusion of some of these substrates would also be a possibility.

7 Determination of Heavy Atom Kinetic Isotope Effects

Heavy atom kinetic isotope effects (HAKIEs) are most commonly determined by means of competitive methods in which both isotopologues are present simultaneously in the reaction solution. Direct comparison of the isotopic reaction rates, which is the usual practice for hydrogen KIEs, is seldom applied as the typical errors in a rate determination are likely to obscure the small HAKIEs. Inter-experimental variation, for example in temperature and contaminants, may not be critical in competitive kinetics as both isotopologues experience the same environment. Moreover, there is no need for isotopically pure substrates as the KIE can be determined using reactants at natural abundance or with labelled reactant(s) at trace amounts.

Depending on whether the reactant or the product is monitored, the KIE can be calculated according to the expression given in Eq. (7.1) or (7.2).

$$KIE = \ln(1-f)/\ln[(1-f)(R_s/R_0)] \quad (7.1)$$

$$KIE = \ln(1-f)/\ln(1-f\,R_p/R_0) \quad (7.2)$$

The fraction of reaction, *f*, is a measure of the extent of conversion of the reaction with the light isotopologue. R_s and R_p are the isotopic ratios at a fraction of reaction, *f*, for the reactant and the product, respectively. The isotopic ratio at 0% conversion is denoted R_0. In order to ensure minimal contribution to the KIE from the error arising from the determination of *f*, the reaction should be stopped at an early stage, i.e. $f < 15\%$, if the isotopic ratios of the product are used. For the same reason, a conversion of about 50% is desirable when the isotopic ratios of the reactant are utilized.[28,121] In practice, this may be in conflict with the investigated system causing the fraction of reaction in the experiment to deviate substantially from the ideal situation. In fact, it is advisable to have a spread of fractions of reaction in an experimental series in order to ensure that the observed KIE is independent on *f*.[121]

7.1 The Nitrogen Kinetic Isotope Effect at Natural Abundance (Paper V)

7.1.1 Experimental Procedure for the Determination of $^{15}(V/K)$

The determination of $^{15}(V/K)$ for the deamination of benzylamine by MAO B was performed with competitive kinetics under steady-state conditions. The reaction medium (containing HEPES 50 mM, Triton (X-100 reduced) 0.5% and semicarbazide hydrochloride 7 mM) was checked for impurities using HPLC before the addition of benzylamine hydrochloride (resulting concentration: 6 mM) after which it was saturated with air and adjusted to pH 7.5 (HCl/KOH). Both the reaction medium and the benzyl alcohol standard solution (12 mM in 50% MeOH in water) were prepared fresh on the day of the experiment.

An aliquot of enzyme (recombinant human liver MAO B) solution was added to the reaction medium tempered to 25.0 ºC. After mixing, the vial was returned to the temperature bath at 25.0 °C and left to react for 35–65 min before quenching with concentrated HCl. The reaction time was adjusted so that 15–20% conversion of the benzylamine was achieved.

In order to assess the fraction of reaction, *f*, unreacted and quenched reaction solution were treated according to the left-hand procedure in Figure 7.1: A 0.5 mL aliquot of the reaction solution was combined with a 0.25 mL portion of the standard solution of benzyl alcohol. The amounts of the combined solutions were monitored by weight rather than volume to ensure high accuracy. Three aliquots of the resulting mixture were successively injected into an HPLC system and the peak areas in the UV chromatograms were averaged. The ratio of the benzylamine and benzyl alcohol concentrations was determined via a standard curve relating the relative peak areas to the relative concentrations. In combination with the weighed quantities of the reactant and standard solutions this yielded the fraction of reaction.

The right-hand procedure in Figure 7.1 describes the determination of the isotopic ratios before and after reaction. A 1.6 mL portion of the reaction solution was injected into a preparative HPLC system. The benzylamine fraction was collected after which the solvent was removed by means of freeze-drying. The solid residual of the fraction was packed in a tin capsule, which was placed in a capped vial to avoid contamination of the sample. Isotope ratio mass spectrometry (IRMS) at natural abundance was performed at the Department of Forest Ecology, Swedish University of Agricultural Sciences, Umeå. The amount of benzylamine used ensured a sufficient amount of nitrogen in each sample (f = 0, 125 μg nitrogen; f = 0.2, 100 μg nitrogen). The KIE was calculated according to Eq. (7.1).

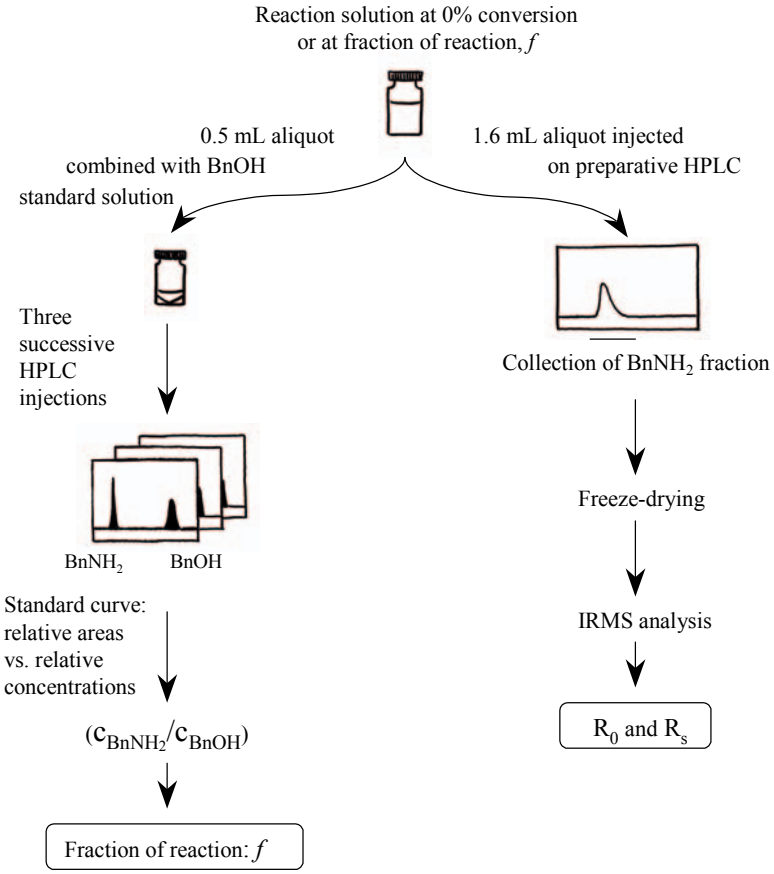

Figure 7.1 The experimental procedure for the determination of $^{15}(V/K)$ for the deamination of benzylamine by MAO B. $BnNH_2$ and BnOH denote benzylamine and benzyl alcohol, respectively.

Further Comments on the Experimental Procedure

The semicarbazide hydrochloride was included in order to serve as a benzaldehyde trap preventing any possible back reaction through semicarbazone formation. Special care was taken not to introduce any nitrogen contaminants during the experimental procedure. The nitrogen-containing HEPES buffer, semicarbazide and semicarbazone were well separated from the benzylamine during the chromatographic procedure, according to LC-MS measurements. Due to the possibility of isotopic fractionation during chromatography,[122] the benzylamine collection was carried out by hand and the fraction was extended in order to ensure that all the material was included. In order to show that neither the chromatography nor the freeze-drying affected the $^{14}N/^{15}N$ ratio, several test samples exposed to either method alone or in combination were analysed.

7.2 Kinetic Isotope Effects Employing ^{11}C and ^{14}C (Papers I–III)

7.2.1 The Use of ^{11}C and ^{14}C in Kinetic Isotope Effect Studies

The largest possible relative mass difference for carbon is achieved by using the combination of ^{11}C and ^{14}C in the determination of carbon KIEs. This is advantageous as the observed KIE is maximised as compared to isotope effects arising from the use of other carbon isotopes. Therefore, the use of $^{11}C/^{14}C$ is especially suited for the study of KIEs that are anticipated to be small, e.g. nucleophile KIEs, or the minor changes that might follow a change in solvent or substrate structure.[123] Furthermore, employing radioisotopes enables sensitive and accurate detection by means of scintillation which, compared with IRMS requires less operator knowledge and is more readily available. The disadvantages arising from the choice of nuclide, i.e. ^{11}C, are: *i*) the need for highly specialized equipment, such as a cyclotron and laboratories suitable for working with radioactive nuclides and *ii*) the short half-life ($t_{½}$ = 20.4 min) of ^{11}C, which means that a maximum of about 60 min can be spent on substrate synthesis and purification before starting the kinetic experiment.

Decay Properties of ^{11}C and ^{14}C

The ^{11}C nuclide decays almost exclusively by positron emission, see Figure 7.2. The positron will rapidly encounter an electron and the ensuing annihilation of the two particles will result in two γ-photons being emitted in opposite directions to each other.

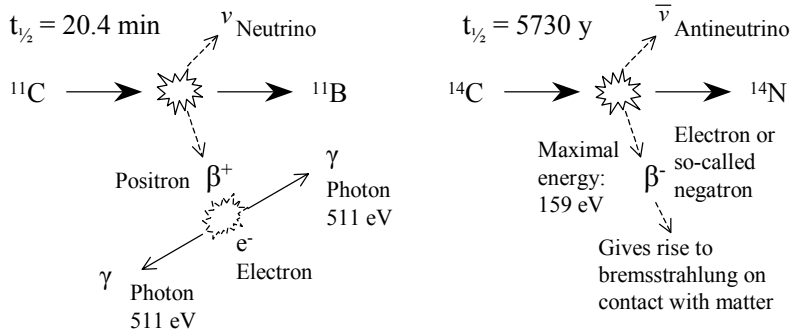

Figure 7.2 The modes of decay and half-lives of ^{11}C and ^{14}C.

This feature is exploited in positron emission tomography (PET) imaging, used in clinical diagnostics as well as physiological research.[124] Therefore, special techniques and synthetic routes have been developed for the synthesis of molecules labelled with positron emitters such as ^{18}F, ^{68}Ga, ^{15}O

and ^{11}C. The other carbon isotope of interest, ^{14}C, has a half-life of 5730 years and is perhaps most widely known for its use in the dating of archaeological findings.[125] As shown in Figure 7.2, ^{14}C decays by β^- emission.

Production of ^{11}C and ^{11}C Precursors

Figure 7.3 shows the production of ^{11}C and some ^{11}C precursors. Nitrogen gas is irradiated with protons accelerated in a cyclotron, which results in a nuclear reaction affording the ^{11}C and an α particle.[126] The highly reactive ^{11}C species combines with trace amounts of oxygen in the target to form [^{11}C]carbon dioxide.[127] An on-line system connected to the cyclotron is utilized for further conversion of the carbon dioxide to either [^{11}C]carbon monoxide or [^{11}C]hydrogen cyanide.[128,129]

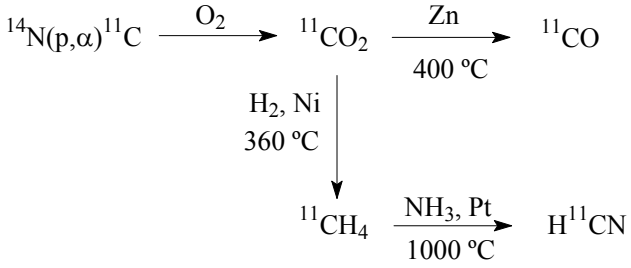

Figure 7.3 The production of ^{11}C via cyclotron-accelerated proton bombardment and some ^{11}C precursors produced via the on-line system connected to the cyclotron unit.

7.2.2 Experimental Procedure for the Determination of $^{11}C/^{14}C$ Kinetic Isotope Effects

The determination of $^{11}C/^{14}C$ KIEs was carried out using a chromatographic procedure in combination with liquid scintillation counting. The procedure for the determination of the nucleophile $^{11}C/^{14}C$ KIE for the reaction of labelled cyanide with some *para*-substituted benzyl chlorides described in Paper II serves as an example for the general kinetic procedure used in all the work with $^{11}C/^{14}C$ (Papers I–III). Further comments regarding the specifics of each piece of work will be given below.

Trapping and Preparation of [^{11}C]Hydrogen Cyanide (Papers II & III)

As can be seen in Figure 7.4, the [^{11}C]hydrogen cyanide is trapped in water at 0 ºC after removal of redundant ammonia from the on-line synthesis by passage through 50% aqueous sulphuric acid. After the addition of [^{14}C]potassium cyanide the solution of labelled cyanide was purified by injection into a preparative HPLC system equipped with a β^+ detector. The

collected HCN fraction was then heated and the hydrogen cyanide gas was transferred into the reaction medium via a gentle stream of nitrogen.

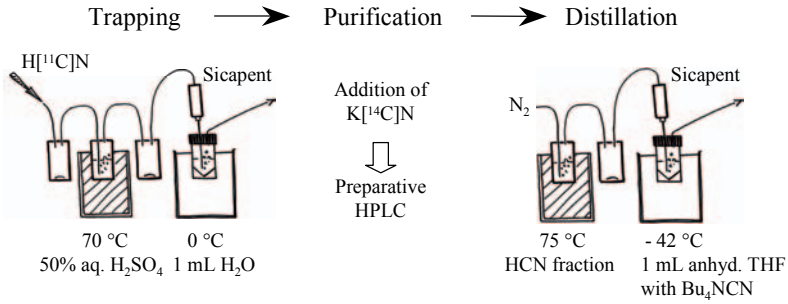

Figure 7.4 Trapping and preparation of the labelled hydrogen cyanide. Sicapent is the commercial name of phosphorus(V) oxide with a moisture indicator added.

Kinetic Procedure

Figure 7.5 depicts the kinetic procedure, which begins with the injection of an aliquot of the cyanide THF solution, containing tetrabutylammonium cyanide and labelled cyanide, into an HPLC system with a β^+ detector. After this, two portions (100 µL and 700 µL) of cyanide solution were transferred into separate vials. A portion of neat *para*-substituted benzyl chloride adjusted to achieve 25–60% conversion of the hydrogen cyanide during the experiment was added to the capped vial containing the 700 µL portion of the cyanide solution. The vial was then placed in a rack connected to a temperature bath at 20.0 °C. Every twenty minutes a sample of reaction mixture was injected into the HPLC equipment and the product fraction was collected. Addition of 20 µL neat *para*-substituted benzyl chloride to the 100 µL portion of cyanide solution at the beginning of the experiment ensured completion of the reaction with respect to cyanide. The fractions of reaction for the injected samples were assessed by the peak areas in the β^+ chromatograms.

Liquid scintillation counting performed immediately after collection of the product fractions gave the combined activity of ^{11}C and ^{14}C. Re-measurement of the fractions on the next day gave the ^{14}C activity. The value of R_0 was based on the collection of the product fraction at full conversion. In order to correct for possible ^{14}C contaminants co-eluting with the products, the initial labelled cyanide solution was analysed twice and fractions were taken corresponding to the product fraction. The mean of these activities together with the earlier collected product fraction of original cyanide solution was subtracted from the ^{14}C activity before use in the calculation of the isotopic ratios, R_0 and R_p. The ^{11}C activity was obtained by subtracting the uncorrected ^{14}C activity from the (^{11}C + ^{14}C) value. After this, the ^{11}C activity was corrected for decay. The KIE was calculated using Eq. (7.2).

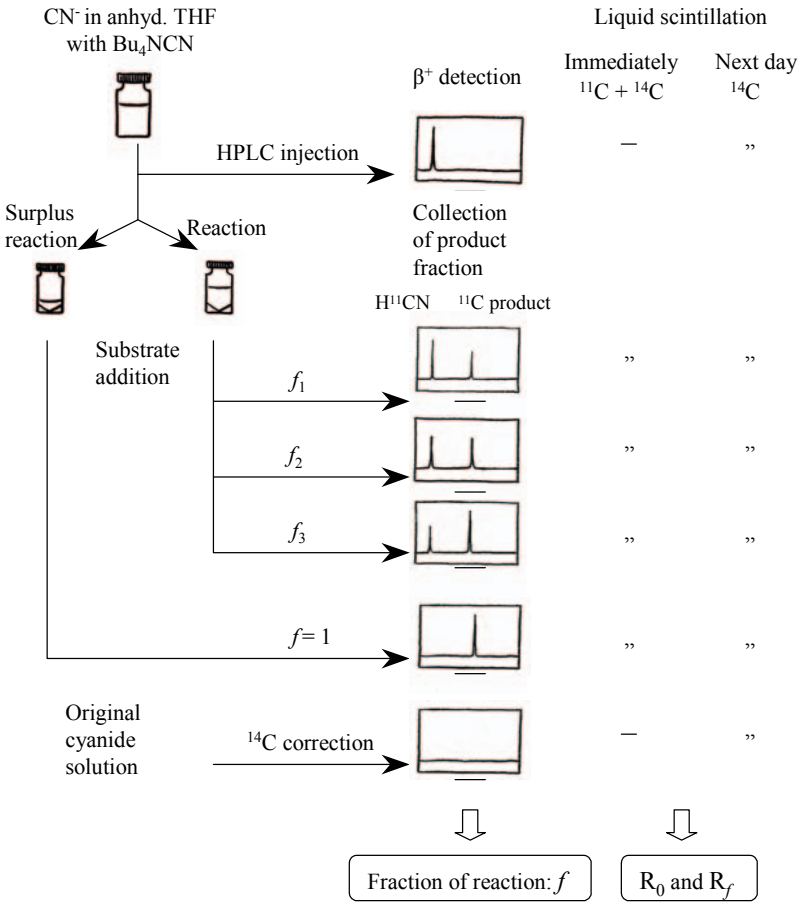

Figure 7.5 The kinetic procedure used for the determination of $^{11}C/^{14}C$ KIEs for the reactions of labelled cyanide with *para*-substituted benzyl chlorides. (Paper II)

Comments on the General Kinetic Procedure (Papers I–III)

The main advantage of using the combination of chromatography and liquid scintillation described above is that only radiochemical purity has to be achieved in the chromatographic procedure. Non-labelled contaminants are acceptable as long as their appearance is regular and the scintillation efficiency is unaffected.

The normal level of radioactivity at the beginning of the kinetic procedure is in the range of 250–150 MBq. The amount of radioactivity and the length of the HPLC procedure together limit the number of times the KIE can be determined in one experiment. The decay of ^{11}C can to some extent be compensated by the injection of larger quantities of the reaction solution, but in the end the activity will be too low to allow β^+ detection of sufficient quality.

Addition of un-labelled reactant, i.e. of the natural abundance isotopic content, is necessary if the rate of the reaction (and thus the observed *f* values within an experiment) is to be controlled. The total concentration of the reactant can be approximated to the concentration given by the un-labelled material as the ^{11}C and ^{14}C are present only at trace amounts.

In order to achieve precise and flexible collection of the HPLC fractions, a manual procedure was employed.

Comments on the Experiments with Labelled Cyanide (Papers II & III)

The major difficulty associated with the labelled cyanide was the fluctuating presence of ^{11}C-labelled by-products formed in the on-line synthesis. It was thought that purification with preparative HPLC solved the problem. However, a remaining ^{11}C impurity was later found to co-elute with the cyanide. As no way of purging the cyanide further was found, the only remaining option was to avoid the impurity as far as possible. This was done by following the isotopic ratio of the product instead of the substrate. The amount of impurity relative to the total activity was established using the chromatogram for the full conversion sample. Thus, the time-corrected absolute area resulting from the impurity could be subtracted from the area of the reactant peak in each calculation of *f*. Usually, the impurity contributed 2.5–0.5% to the total activity. As it was non-reactive and the amount was constant during the experiments, the impurity, although unidentified, was considered not to affect the outcome of the experiments. It should be noted that for experiments with short-lived nuclides the obvious choice is to follow the isotopic ratio of the substrate. Usage of the isotopic ratio of the product involves the need for a fully converted sample (or a pure reactant), which means that there is an uncomfortable trade-off between the time needed for the dead-end reaction to proceed and the decay of ^{11}C. In practice, the solution to this problem was found to be to add surplus substrate to a separate vial containing cyanide solution at the beginning of the experiment. The amount of surplus substrate was calculated to ensure full conversion during the time required for the monitored reaction to reach 50% conversion.

Comments on the Experiments with para-Substituted Benzyl Chlorides (Paper II)

The aldehyde impurities were removed from the *para*-substituted benzyl chlorides by treatment with sodium bisulphite and distillation under reduced pressure.[130,131] Furthermore, the reaction solution was diluted with 30% MeCN in water before injection into the HPLC system. Dilution with water was necessary in order to prevent substantial peak tailing of the HCN, while the acetonitrile was needed to ensure full solubility of the substituted benzyl

cyanides. The fully converted sample was diluted with acetonitrile only to ensure full solubility of the benzyl nitriles.

The initial concentration of both the *para*-methyl and *para*-chlorobenzyl chlorides was approximately 0.07 M, and the concentration of the benzyl chloride was 0.10 M. In all three cases, the initial concentration of the tetrabutylammonium cyanide was 0.05 M.

Comments on the Experiments with Ethyl Substrates (Paper III)

Due to the rapid reaction between the cyanide ion and the ethyl halides in anhydrous DMSO, these substrates were added successively. For example, 7 min after the first addition of ethyl iodide (7 μL, 20 %v/v in DMSO) a cyanide conversion of 30% was attained. An aliquot was then analysed, after which more substrate was added, and so on. For the somewhat slower-reacting ethyl bromide two additions were required, whereas the tosylate was added in one portion. The reactions were slower in 20% aqueous DMSO so all the substrates could be added at once. The conversion of the ethyl tosylate was, however, too slow to be suitable for the study with ^{11}C.

The tetrabutylammonium cyanide concentration in the experiments performed in anhydrous DMSO was 0.1 M. The three successive additions of ethyl iodide resulted in the following concentrations: 0.03 M, 0.015 M and 0.016 M. For ethyl bromide the two successive additions yielded concentrations of 0.03 M and 0.03 M. The single addition of ethyl tosylate resulted in a concentration of 0.08 M.

The initial concentrations of the reactants in 20% aqueous DMSO were approximately 0.065 M and 0.009 M for ethyl iodide and tetrabutylammonium cyanide, respectively. The corresponding concentrations for ethyl bromide and tetrabutylammonium cyanide were approximately 0.280 M and 0.043 M, respectively.

Comments on the Experiments with Labelled Ethyl Chloride (Paper I)

The labelled ethyl chloride was synthesized in the same manner as in a previous study of the reaction between cyanide ions and $^{11}C/^{14}C$-labelled ethyl chloride in DMSO.[45]

In the experiments with labelled ethyl chloride the isotopic ratio of the substrate was monitored. Consequently, the KIE was calculated using Eq. (7.1), but the overall principle of the experiment was as presented in Figure 7.5.

The initial concentrations of ethyl chloride and tetrabutylammonium cyanide were 0.05 M and 0.5 M, respectively.

8 Summary in Swedish

Isotoper i tjänst som mekanismspioner:

Nukleofil bimolekylär substitution och monoaminoxidas B katalys undersökta med kinetiska isotopieffekter för tunga element.

Oj då, redan vid rubriken var det nog en och annan kemiovan som ryckte till och undrade om det är lönt att fortsätta läsa. På ett sätt har ni rätt, detta är inte helt enkelt. Men bara för det, är det inte helt obegripligt.

- Varför är det viktigt att veta hur en kemisk reaktion fungerar?
Detta är av yttersta vikt så snart det finns ett behov av att kontrollera reaktionen. Detaljkunskap om en reaktion gör att vi kan påskynda, stoppa eller styra om reaktionsförloppet efter behag. Mycket av det som vi idag tar för givet som t.ex. tillverkning av plast, färgämnen och läkemedel bygger på att vi förstår hur de kemiska reaktionerna fortskrider och hur vi kan nyttja dem. Det mesta av det som ständigt sker inom oss kan förklaras på en kemisk nivå, vare sig det gäller matspjälkning, DNA-avkodning eller hur nervceller kommunicerar med varandra. Studiet av reaktioner kan även ha en mer grundläggande inrikting då vi försöker reda ut hur och varför molekyler reagerar med varandra och om våra teorier om detta stämmer eller ej.

- Hur går man tillväga?
Det finns många sätt att undersöka hur en reaktion fortskrider (eller som det heter på kemistspråk, att ta reda på en reaktions mekanism). För att lyckas behövs alltid en kombination av fler tillvägagångssätt. Ett av de verktyg som står till förfogande är de så kallade kinetiska isotopieffekterna. Med hjälp av dessa kan man ta reda på om en reaktion sker ett eller fler steg. Ibland går det även att få visshet om i vilken ordning stegen sker i eller vilket av stegen det är som begränsar reaktionens hastighet. Vidare, går isotopieffekten att relatera till skillnaden i struktur mellan reaktanten och övergångstillståndet, vilket måste passeras för att reaktanten skall omvandlas till produkt. De isotopieffekter som rör andra element än väte benämns “isotopieffekter för tunga element”.

- Hur får man fram en kinetisk isotopieffekt?
Här kommer en liten snabbkurs i hur man bestämmer en isotopieffekt:

1. Mät hastigheten för en reaktion.

2. Byt ut en atom i en av reaktanterna mot en isotop av samma grundämne.

3. Mät hastigheten igen för samma reaktion som ovan men nu med den isotopsubstituerade reaktanten.

4. Dividera hastigheten för reaktionen innehållande den lätta isotopen med hastigheten för reaktionen med den tunga isotopen.

5. Om kvoten du fått skiljer sig från ett så har du påvisat en kinetisk isotopieffekt!

- Vad handlar denna avhandling om?
Avhandlingen går att dela in i tre olika delar:

Del 1

I den första delen av avhandlingen har en grundläggande reaktionstyp kallad nukleofil bimolekylär substitution undersökts. Även om denna reaktion är lättbegriplig i teorin och har studerats mycket grundligt genom åren så är det fortfarande inte alltid lätt att förutsäga exakt hur reaktionen påverkas av ett byte av lösningsmedel eller av reaktanternas struktur. Studiet av denna reaktion har haft det dubbla syftet att förbättra förståelsen för förhållandet mellan molekylers struktur och reaktivitet samt att utröna mer om hur de kinetiska isotopieffekterna kan användas.

Del 2

I samtliga studerade reaktioner i del 1 användes cyanidjon som en av reaktanterna. För att få cyanidjoner i lösning tar man lättast ett cyanidsalt och löser upp det i lösningsmedlet. I en del lösningsmedel kommer jonerna att vara helt "fria" (dvs endast i kontakt med lösningsmedlet) medan de i andra förenar sig i så kallade jonpar eller större formationer. Eftersom skillnaden i struktur mellan reaktanten och övergångstillståndet är av betydelse för de kinetiska isotopieffekterna så är det viktigt att veta hur cyanidjonen föreligger. För att ta reda på detta mättes strömledningsförmågan för olika koncentrationer av cyanidsaltet i de

lösningsmedel som var av intresse. Tendensen för jonparning visade sig vara mycket olika stor beroende på lösningsmedelt. Resultaten kan på sikt användas vid tolkningen av de kinetiska isotpieffekterna.

Del 3

I ett försök att få fram avgörande bevis för hur enzymet monoaminoxidas B fungerar bestämdes kväveisotopieffekten för detta enzyms oxidation av bensylamin. Hämmare av monoaminoxidas används bl. a. som antidepressiv medicin och som symptomlindrare vid Parkinsons sjukdom. Vetskapen om hur enzymet fungerar i detalj skulle underlätta formgivningen av nya och bättre hämmare. Tyvärr kunde inte den observerade isotopieffekten användas för att avgöra vilken av de föreslagna mekanismerna som är mest trolig. För att klargöra situationen skulle den nu observerade isotopieffekten behöva jämföras med ytterligare en isotopieffekt av en annan typ.

Acknowledgements

I would like to express my sincere gratitude to my supervisor *Prof. Olle Matsson* for supporting me during these years: Your warmth, sense of humour and subtle leadership have made my work enjoyable!

I would also like to thank:

Prof. Dale E. Edmondson for valuable discussions, enzyme and patience.

Assoc. Prof. Per Beronius for introducing me to the world of conductometry.

Assoc. Prof. Rolf Danielsson for enlightening advice in statistics.

All the S_N2 collaborators: *Prof. Ken C. Westaway, Prof. Raymond A. Poirier* in Canada, *Prof. Piotr Paneth* in Poland and your co-workers.

I am also much obliged to *Prof. Bengt Långström* for allowing me and my group to take advantage of the excellent facilities at the Uppsala Imanet PET Centre and for showing such genuine interest in our research.

Those who have supported me when the cyanide turned foul: *Joachim Schultz, Assoc. Prof. Gunnar Antoni, Fil. lic. Sven-Åke Gustavsson, Daniel Johansen* and all the friendly people in the chemistry laboratory at the Imanet PET Center.

The agencies who have funded my conference trips: *C. F. Liljewalchls resestipendiefond, Svenska Kemistsamfundet* and *the Swedish Science Research Council (VR).*

Jag vill tacka alla er som på något sätt glatt mig under min tid på Kemikum och BMC…

Svante, *Anita* och *Göran*, ni har gjort att OM-gruppen känts lite större! Det är alltid ett nöje att träffa er.

Irina, min trogna följeslagarinna på det ödsliga Gluntenlaboratoriet, vilken tur att du funnits där så att vi har fått lära känna varandra.
–Keep on dancing girl!

Min företrädare, *Per Ryberg*, du sade åt mig att spendera så mycket som möjligt av gruppmedlen för att Olle skulle glömma hur dyr du var i drift. Jag tror att jag har lyckats! Jag kommer alltid att minnas alla de dråpliga och kulinariska upplevelser vi delade i Polen.

Jonas, för alla lyckade samarbeten i hotcellen, både med etylklorid och med frigolit.

Jarle, för alla musiktips och sköna fikastunder.

Det bästa labbet någonsin på Kemikum: Lab. 4016/4017 befolkat av *Anna*, *Cecilia E* (Bakanför), *Stefan B* (–Vadå, den här T-shirten duger väl?), *Ludvig* (–Denna bilen behåller jag min doktorandtid ut!) och *Kalle* (–Jag ska bara koppla in en timer…). Jag saknar er!

Jag vill tillkännage det utmärkta arbete som *Cecilia W*, *Jenny*, *Matthis* och *Jarle* bedrivit då de läst min avhandling. Era synpunkter har varit mycket användbara. Jag tackar även *Helen Sheppard* för en ypperligt genomförd språkgranskning.

Och tack alla ni som givit mig så rar uppmuntran under min kompakta skrivperiod! Tack…
Adolf (Sesamgodis, sena skratt och nysningar),
Henrik (Chips & Livsfilosofi), *Matthis* (Min enda julblomma), *Miranda* (Vackra leenden), *Olle* (“Negerbollar”) och *Lotta* (Hembakat knäckebröd).

Ytterligare några glädjeämnen kemikumtiden fört med sig:
David, *Päivi*, *Judit*, *Eskender*, *Senait*, *Angelica*, *Thavi* och *Takahiro.*

Ni som håller maskineriet i gång:
Eva, *Gunnar*, *Leffe* och *Tomas*.

…och nu till en underbar kvartett: *Cecilia W, Anna, Cecilia E* och *Jenny*.
Ni är som fyra sorters utmärkt champagne jag inte kan sluta dricka! Vilken tur jag har som känner er.

Tack, *Thomas,* min käre vän, vad gjorde jag utan dig? Du har försökt att hålla mig i kontakt med den ickekemiska världen –nu kommer jag ut.

Tack, *Evelina*, min kära vän, nu är det snart dags att du och jag går loss på te och ett paket chockladdoppade kex, eller hur? Jag kan knappt vänta.

Älskade *Mamma* och *Pappa*, tack för uppmuntran och avslappnande sällskap. Jag är så lycklig och tacksam att jag är just er dotter.

Nunc est bibendum, nunc pede libero
pulsanda tellus…

Horatius, Ode 1:37

Uppsala, december 2006

References

(1) Kershaw, D. N.; Leisten, J. A. Alkyl-oxygen fission in ethyl carboxylates. *Proc. Chem. Soc., London* **1960**, 84.

(2) Evans, M. G.; Polanyi, M. Application of the transition-state method to the calculation of reaction velocities, especially in solution. *T. Faraday Soc.* **1935**, *31*, 875-894.

(3) Truhlar, D. G.; Hase, W. L.; Hynes, J. T. Current status of transition-state theory. *J. Phys. Chem.* **1983**, *87*, 2664-2682.

(4) Laidler, K. J.; King, M. C. *J.* Development of transition-state theory. *Phys. Chem-U.S.* **1983**, *87*, 2657-2664.

(5) Eyring, H. Activated complex in chemical reactions. *J. Chem. Phys.* **1935**, *3*, 107-115.

(6) Hammond, G. S. A correlation of reaction rates. *J. Am. Chem. Soc.* **1955**, *77*, 334-338.

(7) More O'Ferrall, R. A. *J. Chem. Soc. B: Physical Organic* **1970**, 274-277.

(8) Jencks, W. P. General acid-base catalysis of complex reactions in water. *Chem. Rev.* **1972**, *72*, 705-718.

(9) Barnes, J. A.; Wilkie, J.; Williams, I. H. Transition-state structural variation and mechanistic change. *J. Chem. Soc., Faraday Trans.* **1994**, *90*, 1709-1714.

(10) Melander, L.; Saunders, W. H., Jr. *Reaction Rates of Isotopic Molecules*; 2 ed.; Wiley-Interscience: New York, 1980.

(11) Shiner, V. J., Jr.; Wilgis, F. P. In *Isotopes in Organic Chemistry*; Buncel, E., Saunders, W. H., Jr., Eds.; Elsevier: New York, 1992; Vol. 8, pp 239-335.

(12) Westheimer, F. H. The magnitude of the primary kinetic isotope effect for compounds of hydrogen and deuterium. *Chem. Rev.* **1961**, *61*, 265-273.

(13) Melander, L. *Isotope Effects on Reaction Rates*; The Ronald Press: New York,1960.

(14) Sühnel, J.; Schowen, R. L. In *Enzyme Mechanism from Isotope Effects*; Cook, P. F., Ed.; CRD Press, Inc.: Boca Ranton, 1991, pp 3-36.

(15) Westaway, K. C. In *Isotopes in Organic Chemistry*; Buncel, E., Lee, C. C., Eds.; Elsevier Science Publishers B. V.: Amsterdam, 1987; Vol. 7, pp 275-392.

(16) Matsson, O.; Westaway, K. C. Secondary deuterium kinetic isotope effects and transition state structure. *Adv. Phys. Org. Chem.* **1998**, *31*, 143-248.

(17) Huskey, W. P. In *Enzyme Mechanism from Isotope Effects*; Cook, P. F., Ed.; CRD Press, Inc.: Boca Ranton, 1991; pp 37-72.
(18) Matsson, O.; Dybala-Defratyka, A.; Rostkowski, M.; Paneth, P.; Westaway, K. C. A theoretical investigation of α-carbon kinetic isotope effects and their relationship to the transition-state structure of S_N2 reactions. *J. Org. Chem.* **2005**, *70*, 4022-4027.
(19) Dybala-Defratyka, A.; Rostkowski, M.; Matsson, O.; Westaway, K. C.; Paneth, P. A new interpretation of chlorine leaving group kinetic isotope effects; A theoretical approach. *J. Org. Chem.* **2004**, *69*, 4900-4905.
(20) Melander, L.; Saunders, W. H., Jr. In *Reaction Rates of Isotopic Molecules*; John Wiley & Sons: New York, 1980; pp 140-152.
(21) Saunders, W. H., Jr. The contribution of tunneling to secondary isotope effects. *Croat. Chem. Acta* **1992**, *65*, 505-515.
(22) Kost, D.; Pross, A. The misuse of energy profiles. *Education in Chemistry* **1977**, *14*, 87-88.
(23) Persson, J.; Matsson, O. Use of fluorine kinetic isotope effects in the study of steric effects in nucleophilic aromatic substitution reactions. *J. Org. Chem.* **1998**, *63*, 9348-9350.
(24) Parkin, D. W. In *Enzyme Mechanism from Isotope Effects*; Cook, P. F., Ed.; CRD Press, Inc.: Boca Ranton, 1991; pp 269-290.
(25) Hermes, J. D.; Weiss, P. M.; Cleland, W. W. *Biochemistry* **1985**, *24*, 2959-2967.
(26) Kurtz, K. A.; Rishavy, M. A.; Cleland, W. W.; Fitzpatrick, P. F. Nitrogen isotope effects as probes of the mechanism of D-amino acid oxidase. *J. Am. Chem. Soc.* **2000**, *122*, 12896-12897.
(27) Ryberg, P.; Matsson, O. The mechanism of base-promoted HF elimination from 4-fluoro-4-(4-nitrophenyl)butan-2-one is E1cB. Evidence from double isotopic fractionation experiments. *J. Org. Chem.* **2002**, *67*, 811-814.
(28) Cleland, W. W. In *Enzyme Mechanism from Isotope Effects*; Cook, P. F., Ed.; CRD Press, Inc.: Boca Ranton, 1991; pp 247-265.
(29) Kresge, A. J. Correlation of kinetic isotope effects with free energies of reaction. *J. Am. Chem. Soc.* **1980**, *102*, 7797-7798.
(30) Ingold, C. K. *Structure and Mechanism in Organic Chemistry*; Cornell University Press: Ithaca, New York, 1953.
(31) Westaway, K. C. Isotope effects in nucleophilic-substitution reactions. 9. The effect of bond strength on substituent effects on the structure of S_N2 transition-states. *Can. J. Chem.* **1993**, *71*, 2084-2094.
(32) Westaway, K. C. Solvent effects on the structure of S_N2 transition states. *Can. J. Chem.* **1978**, *56*, 2691-2699.
(33) Westaway, K. C. Using kinetic isotope effects to determine the structure of the transition state of S_N2 reactions. *Adv. Phys. Org. Chem.* **2006**, *41*, 217-273.

(34) Matsson, O.; Persson, J.; Axelsson, B. S.; Langstrom, B.; Fang, Y.; Westaway, K. C. Using incoming group C-11/C-14 kinetic isotope effects to model the transition states for the S_N2 reactions between *para*-substituted benzyl chlorides and labeled cyanide ion. *J. Am. Chem. Soc.* **1996**, *118*, 6350-6354.
(35) Anderson, V. E.; Cassano, A. G.; Harris, M. E. In *Isotope Effects in Chemistry and Biology*; Kohen, A., Limbach, H.-H., Eds.;Taylor & Francis: Boca Raton, 2006; pp 893-914.
(36) Paneth, P.; O'Leary, M. H. Nitrogen and deuterium isotope effects on quaternization of N,N-dimethyl-p-toluidine. *J. Am. Chem. Soc.* **1991**, *113*, 1691-1693.
(37) Yamataka, H.; Ando, T. Variations of carbon-14 kinetic isotope effects in the Menschutkin type reaction of benzyl arenesulfonates. *Tetrahedron Lett.* **1975**, 1059-1062.
(38) Willi, A. V. In *Isotopes in Organic Chemistry; Buncel, E.; Lee, C. C.;* Elsevier: Amsterdam, 1977; *3*, pp 237-283.
(39) Axelsson, B. S.; Matsson, O.; Langstrom, B. A secondary C-11/C-14-kinetic isotope effect in the base-catalyzed prototropic rearrangement of 1-methylindene to 3-methylindene. *J. Am. Chem. Soc.* **1990**, *112*, 6661-6668.
(40) Poirier, R. A.; Wang, Y. L.; Westaway, K. C. A theoretical-study of the relationship between secondary alpha-deuterium kinetic isotope effects and the structure of S_N2 transition-states. *J. Am. Chem. Soc.* **1994**, *116*, 2526-2533.
(41) Barnes, J. A.; Williams, I. H. Theoretical investigation of the origin of secondary a-deuterium kinetic isotope effects. *J. Chem. Soc., Chem. Commun.* **1993**, 1286-1287.
(42) Davico, G. E.; Bierbaum, V. M. Reactivity and Secondary Kinetic Isotope Effects in the S_N2 Reaction Mechanism: Dioxygen Radical Anion and Related Nucleophiles. *J. Am. Chem. Soc.* **2000**, *122*, 1740-1748.
(43) Westaway, K. C.; VanPham, T.; Fang, Y. R. Using secondary alpha deuterium kinetic isotope effects to determine the symmetry of S_N2 transition states. *J. Am. Chem. Soc.* **1997**, *119*, 3670-3676.
(44) Hengge, A. C. In *Isotope Effects in Chemistry and Biology*; Kohen, A., Limbach, H.-H., Eds.; Taylor & Francis: Boca Raton, 2006; pp 955-974.
(45) Fang, Y.-r.; Gao, Y.; Ryberg, P.; Eriksson, J.; Kolodziejska-Huben, M.; Dybala-Defratyka, A.; Madhavan, S.; Danielsson, R.; Paneth, P.; Matsson, O.; Westaway, K. C. Experimental and theoretical multiple kinetic isotope effects for an S_N2 reaction. An attempt to determine transition-state structure and the ability of theoretical methods to predict experimental kinetic isotope effects. *Chem. Eur. J.* **2003**, *9*, 2696-2709.
(46) Bogdanov, B.; McMahon, T. B. Thermochemistry and structures of solvated S_N2 complexes and transition states in the gas phase: experiment and theory. *Int. J. Mass Spectrom.* **2005**, *241*, 205-223.

(47) Gordon, A. J.; Ford, R. A. In *The Chemist's Companion*; J. Wiley and Sons: New York, 1972, pp 6-7.
(48) Almerindo, G. I.; Pliego, J. R. A initio study of the S_N2 and E2 mechanisms in the reaction between the cyanide ion and ethyl chloride in dimethyl sulfoxide solution. *Org. Lett.* **2005**, *7*, 1821-1823.
(49) Yamataka, H.; Aida, M. An ab initio MO study on the hydrolysis of methyl chloride with explicit consideration of 13 water molecules. *Chem. Phys. Lett.* **1998**, *289*, 105-109.
(50) Mohamed, A. A.; Jensen, F. Steric Effects in S_N2 Reactions. The Influence of Microsolvation. *J. Phys. Chem. A* **2001**, *105*, 3259-3268.
(51) Fry, A. in *Isotope Effects in Organic Chemistry*, Collins, C. J. J., Bowman, N. S., Eds.; A.C.S. Monograph 167; Van Nostrand Reinhold: New York, 1970; p 380.
(52) Hill, J. W.; Fry, A. Chlorine isotope effects in the reactions of benzyl and substituted benzyl chlorides with various nucleophiles. *J. Am. Chem. Soc.* **1962**, *84*, 2763-2769.
(53) Grimsrud, E. P. Chlorine kinetic isotope effects in nucleophilic displacement reactions. Ph.D. Thesis, University of Wisconsin, Madison, WI, USA, 1971.
(54) Koerner, T.; Fang, Y. R.; Westaway, K. C. Using incoming nucleophile primary hydrogen-deuterium kinetic isotope effects to model the S_N2 transition state. *J. Am. Chem. Soc.* **2000**, *122*, 7342-7350.
(55) Westaway, K. C.; Waszczylo, Z. Isotope effects in nucleophilic substitution reactions. IV. The effect of changing a substituent at the α-carbon on the structure of S_N2 transition states. *Can. J. Chem.* **1982**, *60*, 2500-2520.
(56) Westaway, K. C.; Fang, Y. R.; Persson, J.; Matsson, O. Using C-11/C-14 incoming group and secondary alpha-deuterium KIEs to determine how a change in leaving group alters the structure of the transition state of the S_N2 reactions between m-chlorobenzyl *para*-substituted benzenesulfonates and cyanide ion. *J. Am. Chem. Soc.* **1998**, *120*, 3340-3344.
(57) Fuoss, R. M.; Kraus, C. A. Properties of electrolytic solutions. IV. The conductance minimum and the formation of triple ions due to the action of Coulomb forces. *J. Am. Chem. Soc.* **1933**, *55*, 2387-2399.
(58) Robinson, R. A.; Stokes, R. H. *Electrolyte Solutions*; 2 ed.; Dover Publications, Inc.: New York, 1959; pp 87-102.
(59) Robinson, R. A.; Stokes, R. H. *Electrolyte Solutions*; 2 ed.; Dover Publications, Inc.: New York, 1959; pp 133-134.

(60) Jones, G.; Josephs, R. C. The measurement of the conductance of electrolytes. I. An experimental and theoretical study of principles of design of the Wheatstone bridge for use with alternating currents and an improved form of direct-reading alternating-current bridge. *J. Am. Chem. Soc.* **1928**, *50*, 1049-1092.
(61) Daggett, H. M., Jr.; Bair, E. J.; Kraus, C. A. Properties of electrolytic solutions. XLVII. Conductance of some quaternary ammonium and other salts in water at low concentration. *J. Am. Chem. Soc.* **1951**, *73*, 799-803.
(62) Lind, J. E., Jr.; Zwolenik, J. J.; Fuoss, R. M. Calibration of conductance cells at 25 ºC with aqueous solutions of potassium chloride. *J. Am. Chem. Soc.* **1959**, *81*, 1557-1559.
(63) Fernandez-Prini, R. Conductance of electrolyte solutions. Modified expression for its concentration dependence. *Trans. Faraday Soc.* **1969**, *65*, 3311-3313.
(64) Fuoss, R. M.; Hsia, K.-L. Association of 1-1 salts in water. *Proc. Natl. Acad. Sci. U.S. A.* **1967**, *57*, 1550-1557.
(65) Hsia, K.-L.; Fuoss, R. M. Conductance of the alkali halides. XI. Cesium bromide and iodide in water at 25 ºC. *J. Am. Chem. Soc.* **1968**, *90*, 3055-3060.
(66) Robinson, R. A.; Stokes, R. H. *Electrolyte Solutions*; 2 ed.; Dover Publications, Inc.: New York, 1959; pp 392-431.
(67) Fuoss, R. M.; Accascina, F. *Electrolytic Conductance*; Interscience Publishers, Inc.: New York, 1959.
(68) Robinson, R. A.; Stokes, R. H. *Electrolyte Solutions*; 2 ed.; Dover Publications, Inc.: New York; 1959.
(69) Riddick, J. A.; Bunger, W. B. *Techniques of Chemistry, Vol. II, Organic Solvents*; Wiley-Interscinence: New York; 1970.
(70) *Tables of interatomic distances and configuration in molecules and ions*; the Chemical Society: Burlington House, London, W.1; 1958.
(71) Accascina, F.; Goffredi, M.; Triolo, R. Ion-pair formation of quaternary ammonium salts in hydrogen-bonded solvents. Electrical conductivities of some tetraalkylammonium perchlorates in water-dioxane mixtures at 25 ºC. *Z. Phys. Chem. (Munich)* **1972**, *81*, 148-157.
(72) Hughes, E. D.; Ingold, C. K.; Patai, S.; Pocker, Y. Mechanism of substitution at a saturated carbon atom. LIII. Conductances of some quaternary ammonium salts in benzene, as a preliminary to the study of unimolecular nucleophilic substitution in that solvent. *J. Chem. Soc.* **1957**, 1206-1219.
(73) Beronius, P.; Pataki, L. On the study of triple ion formation. Sodium iodide in 1-octanol at 25 ºC. *Acta Chim. Hung.* **1980**, *103*, 17-25.
(74) Beronius, P.; Lindbaeck, T. On the study of triple ion formation. Electrolytes forming only one kind of triplet. *Acta Chem. Scand. A* **1979**, *A33*, 397-399.

(75) Berry, M. D.; Juorio, A. V.; Paterson, I. A. The functional role of monoamine oxidases A and B in the mammalian central nervous system. *Prog. Neurobiol.* **1994**, *42*, 375-391.
(76) Massey, V. The chemical and biological versatility of riboflavin. *Biochem. Soc. Trans.* **2000**, *28*, 283-296.
(77) Johnston, J. P. Some observations on a new inhibitor of monoamine oxidase in brain tissue. *Biochem. Pharmacol.* **1968**, *17*, 1285-1297.
(78) Bach, A. W.; Lan, N. C.; Johnson, D. L.; Abell, C. W.; Bembenek, M. E.; Kwan, S. W.; Seeburg, P. H.; Shih, J. C. cDNA cloning of human liver monoamine oxidase A and B: molecular basis of differences in enzymatic properties. *P. Natl. Acad. Sci. U.S. A.* **1988**, *85*, 4934-4938.
(79) Youdim, M. B. H.; Edmondson, D.; Tipton, K. F. The therapeutic potential of monoamine oxidase inhibitors. *Nat. Rev. Neurosci.* **2006**, *7*, 295-309.
(80) Special issue on Monoamine Oxidase. *NeuroToxicology* **2004**, *25*, 1-338.
(81) Pietrangeli, P.; Mondovi, B. Amine Oxidases and Tumors. *NeuroToxicology* **2004**, *25*, 317-324.
(82) Edelstein, S. B.; Breakefield, X. O. Monoamine oxidases A and B are differentially regulated by glucocorticoids and "aging" in human skin fibroblasts. *Cell. Mol. Neurobiol.* **1986**, *6*, 121-50.
(83) Vindis, C.; Seguelas, M.-H.; Bianchi, P.; Parini, A.; Cambon, C. Monoamine oxidase B induces ERK-dependent cell mitogenesis by hydrogen peroxide generation. *Biochem. Bioph. Res. Co.* **2000**, *271*, 181-185.
(84) Oreland, L. Platelet Monoamine Oxidase, Personality and alcoholism: The rise, fall and resurrection. *NeuroToxicology* **2004**, *25*, 79-89.
(85) Herraiz, T.; Chaparro, C. Human monoamine oxidase enzyme inhibition by coffee and β-carbolines norharman and harman isolated from coffee. *Life Sci.* **2006**, *78*, 795-802.
(86) Castagnoli, K.; Murugesan, T. Tobacco leaf, smoke and smoking, MAO inhibitors, Parkinson's disease and neuroprotection; Are there links? *NeuroToxicology* **2004**, *25*, 279-291.
(87) Ramsay, R. R. Kinetic mechanism of monoamine oxidase A. *Biochemistry* **1991**, *30*, 4624-4629.
(88) Edmondson, D. E.; Mattevi, A.; Binda, C.; Li, M.; Hubalek, F. Structure and mechanism of monoamine oxidase. *Curr. Med. Chem.* **2004**, *11*, 1983-1993.
(89) Miller, J. R.; Edmondson, D. E. Influence of flavin analogue structure on the catalytic activities and flavinylation reactions of recombinant human liver monoamine oxidases A and B. *Biochemistry* **1999**, *38*, 13670-13683.
(90) Jonsson, T.; Edmondson, D. E.; Klinman, J. P. Hydrogen tunneling in the flavoenzyme monoamine-oxidase-B. *Biochemistry* **1994**, *33*, 14871-14878.

(91) De Colibus, L.; Li, M.; Binda, C.; Lustig, A.; Edmondson, D. E.; Mattevi, A. Three-dimensional structure of human monoamine oxidase A (MAO A): Relation to the structures of rat MAO A and human MAO B. *P. Natl. Acad. Sci. U.S.A.* **2005**, *102*, 12684-12689.
(92) Nandigama, R. K.; Edmondson, D. E. Influence of FAD structure on its binding and activity with the C406A mutant of recombinant human liver monoamine oxidase A. *Biochemistry* **2000**, *39*, 15258-15265.
(93) Walker, M. C.; Edmondson, D. E. Structure-activity-relationships in the oxidation of benzylamine analogs by bovine liver mitochondrial monoamine-oxidase-B. *Biochemistry* **1994**, *33*, 7088-7098.
(94) Newton-Vinson, P.; Hubalek, F.; Edmondson, D. E. High-level expression of human liver monoamine oxidase B in Pichia pastoris. *Protein Expres. Purif.* **2000**, *20*, 334-345.
(95) Husain, M.; Edmondson, D. E.; Singer, T. P. Kinetic studies on the catalytic mechanism of liver monoamine oxidase. *Biochemistry* **1982**, *21*, 595-600.
(96) Binda, C.; Hubalek, F.; Li, M.; Herzig, Y.; Sterling, J.; Edmondson, D. E.; Mattevi, A. Crystal structures of monoamine oxidase B in complex with four inhibitors of the N-propargylaminoindan class. *J. Med. Chem.* **2004**, *47*, 1767-1774.
(97) Binda, C.; Li, M.; Hubalek, F.; Restelli, N.; Edmondson, D. E.; Mattevi, A. Insights into the mode of inhibition of human mitochondrial monoamine oxidase B from high-resolution crystal structures. *Proc. Natl. Acad. Sci. U.S.A.* **2003**, *100*, 9750-9755.
(98) Binda, C.; Newton-Vinson, P.; Hubalek, F.; Edmondson, D. E.; Mattevi, A. Structure of human monoamine oxidase B, a drug target for the treatment of neurological disorders. *Nat. Struct. Biol.* **2002**, *9*, 22-26.
(99) Ma, J. C.; Yoshimura, M.; Yamashita, E.; Nakagawa, A.; Ito, A.; Tsukihara, T. Structure of rat monoamine oxidase A and its specific recognitions for substrates and inhibitors. *J. Mol. Biol.* **2004**, *338*, 103-114.
(100) Binda, C.; Hubalek, F.; Li, M.; Edmondson, D. E.; Mattevi, A. Crystal structure of human monoamine oxidase B, a drug target enzyme monotopically inserted into the mitochondrial outer membrane. *FEBS Lett.* **2004**, *564*, 225-228.
(101) Hubalek, F.; Binda, C.; Khalil, A.; Li, M.; Mattevi, A.; Castagnoli, N.; Edmondson, D. E. Demonstration of isoleucine 199 as a structural determinant for the selective inhibition of human monoamine oxidase B by specific reversible inhibitors. *J. Biol. Chem.* **2005**, *280*, 15761-15766.
(102) Binda, C.; Mattevi, A.; Edmondson, D. E. Structure-function relationships in flavoenzyme-dependent amine oxidations. A comparison of polyamine oxidase and monoamine oxidase. *J. Biol. Chem.* **2002**, *277*, 23973-23976.

(103) Vintem, A. P. B.; Price, N. T.; Silverman, R. B.; Ramsay, R. R. Mutation of surface cysteine 374 to alanine in monoamine oxidase A alters substrate turnover and inactivation by cyclopropylamines. *Bioorg. Med. Chem.* **2005**, *13*, 3487-3495.
(104) Lu, X.; Rodriguez, M.; Ji, H.; Silverman, R. B.; Vintem, A. P. B.; Ramsay, R. R. In *Flavins and Flavoproteins 2002, Proceedings of the International Symposium, 14th, Cambridge, United Kingdom, July 14-18, 2002*; Chapman, S., Perham, R., Scrutton, N. S., Eds.; Rudolf Weber Agency for Scientific Publications, Berlin: 2002, pp 817-830.
(105) Silverman, R. B.; Hoffman, S. J.; Catus, W. B., III A mechanism for mitochondrial monoamine oxidase catalyzed amine oxidation. *J. Am. Chem. Soc.* **1980**, *102*, 7126-7128.
(106) Silverman, R. B. In *The Organic Chemistry of Enzyme-Catalyzed Reactions*; Academic Press: San Diego, 2000; pp 132-141.
(107) Rimoldi, J. M.; Puppali, S. G.; Isin, E.; Bissel, P.; Khalil, A.; Castagnoli, N. A novel and selective monoamine oxidase B substrate. *Bioorg. Med. Chem.* **2005**, *13*, 5808-5813.
(108) Rigby, S. E. J.; Hynson, R. M. G.; Ramsay, R. R.; Munro, A. W.; Scrutton, N. S. Flavoenzyme catalysed oxidation of amines: roles for flavin and protein-based radicals. *J. Biol. Chem.* **2005**, *280*, 4627-4631.
(109) Ramsay, R. R.; Upadhyay, A. K.; Li, M.; Edmondson, D. E. In *Flavin and Flavoproteins 2005*; *Proceedings of the International Symposium, 15th, Kanagawa, Japan, April 17-22, 2005*; Nishino, T., Miura, R., Tanokure, M., Eds.; ARchitect Inc. Tokyo: 2005, pp 137-142.
(110) Miller, J. R.; Edmondson, D. E.; Grissom, C. B. Mechanistic probes of monoamine-oxidase-B catalysis - rapid-scan stopped-flow and magnetic-field independence of the reductive half-reaction. *J. Am. Chem. Soc.* **1995**, *117*, 7830-7831.
(111) Edmondson, D. E.; Bhattacharyya, A. K.; Walker, M. C. Spectral and kinetic-studies of imine product formation in the oxidation of *p*-(N,N-dimethylamino)benzylamine analogs by monoamine oxidase-B. *Biochemistry* **1993**, *32*, 5196-5202.
(112) Yu, P. H. 3 Types of stereospecificity and the kinetic deuterium-isotope effect in the oxidative deamination of dopamine as catalyzed by different amine oxidases. *Biochem. Cell Biol.* **1988**, *66*, 853-861.
(113) Kim, J. M.; Bogdan, M. A.; Mariano, P. S. Mechanistic analysis of the 3-methyllumiflavin-promoted oxidative deamination of benzylamine - A potential model for monoamine-oxidase catalysis. *J. Am. Chem. Soc.* **1993**, *115*, 10591-10595.
(114) Hoegy, S. E.; Mariano, P. S. Mechanistic and synthetic aspects of amine oxidations promoted by 3-methyl-5-ethyllumiflavinium perchlorate. *Tetrahedron* **1997**, *53*, 5027-5046.

(115) Erdem, S. S.; Karahan, O.; Yildiz, I.; Yelekci, K. A computational study on the amine-oxidation mechanism of monoamine oxidase: Insight into the polar nucleophilic mechanism. *Org. Biomol. Chem.* **2006**, *4*, 646-658.
(116) McEwen, C. M., Jr.; Sasaki, G.; Lenz, W. R., Jr. Human liver mitochondrial monoamine oxidase. I. Kinetic studies of model interactions. *J. Biol. Chem.* **1968**, *243*, 5217-5225.
(117) Edmondson, D. E.; Bhattacharrya, A. K.; Xu, J. J. Evidence for alternative binding modes in the interaction of benzylamine analogues with bovine liver monoamine oxidase B. *BBA-Protein Struct. M.* **2000**, *1479*, 52-58.
(118) Fossey, J.; Lefort, D.; Sorba, J. *Free Radicals in Organic Chemistry*; Wiley & Sons: Chichester, 1995.
(119) Kresge, A. J.; Lichtin, N. N.; Rao, K. N.; Weston, R. E., Jr. Ionization and dissociation equilibriums in liquid sulfur dioxide. X. The primary carbon isotope effect on the ionization of triphenylmethyl chloride. Experimental determination, theoretical justification, and implications for carbon isotope effects on nucleophilic substitution at saturated carbon. *J. Am. Chem. Soc.* **1965**, *87*, 437-445.
(120) Amundsen, L. H.; Nelson, L. S. Reduction of nitriles to primary amines with lithium aluminum hydride. *J. Am. Chem. Soc.* **1951**, *73*, 242-244.
(121) Paneth, P. In *Isotopes in Organic Chemistry*; Buncel, E., Saunders, W. H., Jr., Eds.; Elsevier: New York, 1992; Vol. 8, pp 41-68.
(122) Filer, C. N. Isotopic fractionation of organic compounds in chromatography. *J. Labelled Compd. Rad.* **1999**, *42*, 169-197.
(123) Matsson, O. In *Isotope Effects in Chemistry and Biology*; Kohen, A., Limbach, H.-H., Eds.; Taylor & Francis: Boca Raton, 2006; pp 417-432.
(124) Phelps, M. E. Inaugural Article: Positron emission tomography provides molecular imaging of biological processes. *P. Natl. Acad. Sci. U.S.A.* **2000**, *97*, 9226-9233.
(125) Schwarcz, H. P. Chronometric Dating in Archaeology: A Review. *Acc. Chem. Res.* **2002**, *35*, 637-643.
(126) Bida, G. T.; Ruth, T. J.; Wolf, A. P. Experimentally determined thick target yields for the $^{14}N(p,\alpha)^{11}C$ reaction. *Radiochim. Acta* **1980**, *27*, 181-185.
(127) Ache, H. J.; Wolf, A. P. Effect of radiation on the reactions of recoil carbon-11 in the nitrogen-oxygen system. *J. Phys. Chem.* **1968**, *72*, 1988-1993.
(128) Christman, D. R.; Finn, R. D.; Karlstrom, K. I.; Wolf, A. P. Production of ultrahigh activity carbon-11-labeled hydrogen cyanide, carbon dioxide, carbon monoxide, and methane via the $^{14}N(p,\alpha)^{11}C$ reaction. XV. *Int. J. Appl. Radiat. Is.* **1975**, *26*, 435-442.

(129) Iwata, R.; Ido, T.; Takahashi, T.; Nakanishi, H.; Iida, S. Optimization of [^{11}C]HCN production and no-carrier-added [1-^{11}C]amino acid synthesis. *Appl. Radiat. Isotopes* **1987**, *38*, 97-102.
(130) Shiner, R. L.; Fuson, R. L.; Curtin, D. Y. In *The Systematic Identification of Organic Compounds*; 4 ed.; Wiley & Sons: New York, 1959; p 149.
(131) Perrin, D. D.; Armarego, W. L. F. *Purifications of Laboratory Chemicals*; 3 ed.; Pergamon Press: Oxford, 1988, pp 60-61, 367.

Acta Universitatis Upsaliensis

Digital Comprehensive Summaries of Uppsala Dissertations from the Faculty of Science and Technology 265

Editor: The Dean of the Faculty of Science and Technology

A doctoral dissertation from the Faculty of Science and Technology, Uppsala University, is usually a summary of a number of papers. A few copies of the complete dissertation are kept at major Swedish research libraries, while the summary alone is distributed internationally through the series Digital Comprehensive Summaries of Uppsala Dissertations from the Faculty of Science and Technology. (Prior to January, 2005, the series was published under the title "Comprehensive Summaries of Uppsala Dissertations from the Faculty of Science and Technology".)

Distribution: publications.uu.se
urn:nbn:se:uu:diva-7441

ACTA
UNIVERSITATIS
UPSALIENSIS
UPPSALA
2006